University of Minnesota
ST. ANTHONY FALLS HYDRAULIC LABORATORY

Project Report No. 143

A Physical Model Study of the MAIN INTERCEPTOR DIVERSION STRUCTURE AT THE EXPANDED METROPOLITAN WASTEWATER TREATMENT PLANT

by
Heinz Stefan,
Earl Bancroft,
and
Glenn Martin

Prepared for
TOLTZ, KING, DUVALL, ANDERSON and ASSOCIATES, INC.
St. Paul, Minnesota
and the
METROPOLITAN SEWER BOARD

June 1973
Minneapolis, Minnesota

CONTENTS

I. INTRODUCTION

Projections of the volume of sewage flow into the Metropolitan Wastewater Treatment Plant (Pig's Eye plant) serving the Minneapolis-St. Paul metropolitan area have compelled the Metropolitan Sewer Board to plan an expansion of the existing treatment facilities at Pig's Eye Island on the Mississippi River. A listing of selected anticipated flows is given in Table A-1 of Appendix A. Under the title "Project 71" it is planned to increase the pretreatment and primary treatment capacity from an existing 260 MGD design capacity to 620 MGD, which corresponds to the present interceptor capacity. The increment of 360 MGD will be treated in new and separate facilities to be located to the east of the existing ones. To route part of the flow to the new facilities, a diversion (division) structure in the main interceptor just north of the existing plant is projected.

II. OBJECTIVE OF STUDY

It is the objective of the model study described herein to examine a proposed design for the diversion structure and, if necessary, recommend changes in that design. The criteria to be used are an equitable distribution of the flow of water and grit between the old and the new parts of the plant and acceptable hydraulic conditions (depths of flow, velocities, energy losses, etc.) at the structure.

Because the flow through the division structure is of a complicated three-dimensional nature and involves flow separations and reattachments, large eddies, secondary currents, and standing waves in addition to grit transport, it was necessary to build a physical laboratory model of the structure. No analytical methods are available for studying the simultaneous occurrence of these phenomena and their effects.

An inadequate design of the diversion structure could result in hydraulic flow conditions such that the total flow would not be divided in the desired proportions. The flow through the existing treatment facilities and the projected expanded facilities is a gravity flow system, and it is anticipated that the distribution of the total flow can be achieved by operating control devices, probably weirs, at the old and the new facility. The model study will show which flow depths at the end of the diversion canal

have to be provided to assure an equitable distribution of the water by downstream control.

The flow of water and the flow of grit (bed load) through a diversion structure are related, but are by no means proportional to each other. It is very probable that in the diversion structure the grit load will not be divided in the same proportions as the water flow. It is desired to route approximately 58 per cent of the total sewage flow and more than 50 per cent of the total grit load toward the new facilities. Only physical experiments can show whether and how such a distribution can be achieved.

The division or diversion of water planned for the Metropolitan Wastewater Treatment Plant is similar to the diversions found in large-scale irrigation projects. It is widely recognized that the design of diversions in free surface gravity flow systems requires particular care if sediment is to be either kept out of a diversion canal or moved into it, depending on the circumstances. Physical model studies are always made if an appropriate distribution of water and sediment is a critical requirement.

III. BACKGROUND INFORMATION

The projected diversion structure will replace a 158 ft long section of the existing main interceptor canal. The diverted flow will be routed through a 90° bend with a 100 ft radius into a straight combined interceptor section. The proposed design is shown in Fig. 1 and a cross section through the existing main interceptor in Fig. 2. Other hydraulic characteristics of the combined interceptor are given in Appendix A, Table A-2. The flow rates and depths are from Table A-1. The friction factor f is obtained from the Colebrook-White formula (Moody-Diagram) for an absolute roughness value of $k = 0.004$ ft. The friction factors obtained in this manner are slightly higher than those found from measurements in new concrete pipes (Ref. [1]*, p. 67).

The flow depths at the location of the projected diversion structure are affected by a downstream control in the form of an overfall (weir) at the end of the existing settling chambers and a similar device to be installed in the projected portion of the plant. Backwater curve computations carried out by Toltz, King, Duvall, Anderson and Assoc., Inc., have provided the

*Numbers in brackets refer to list of references on page 26.

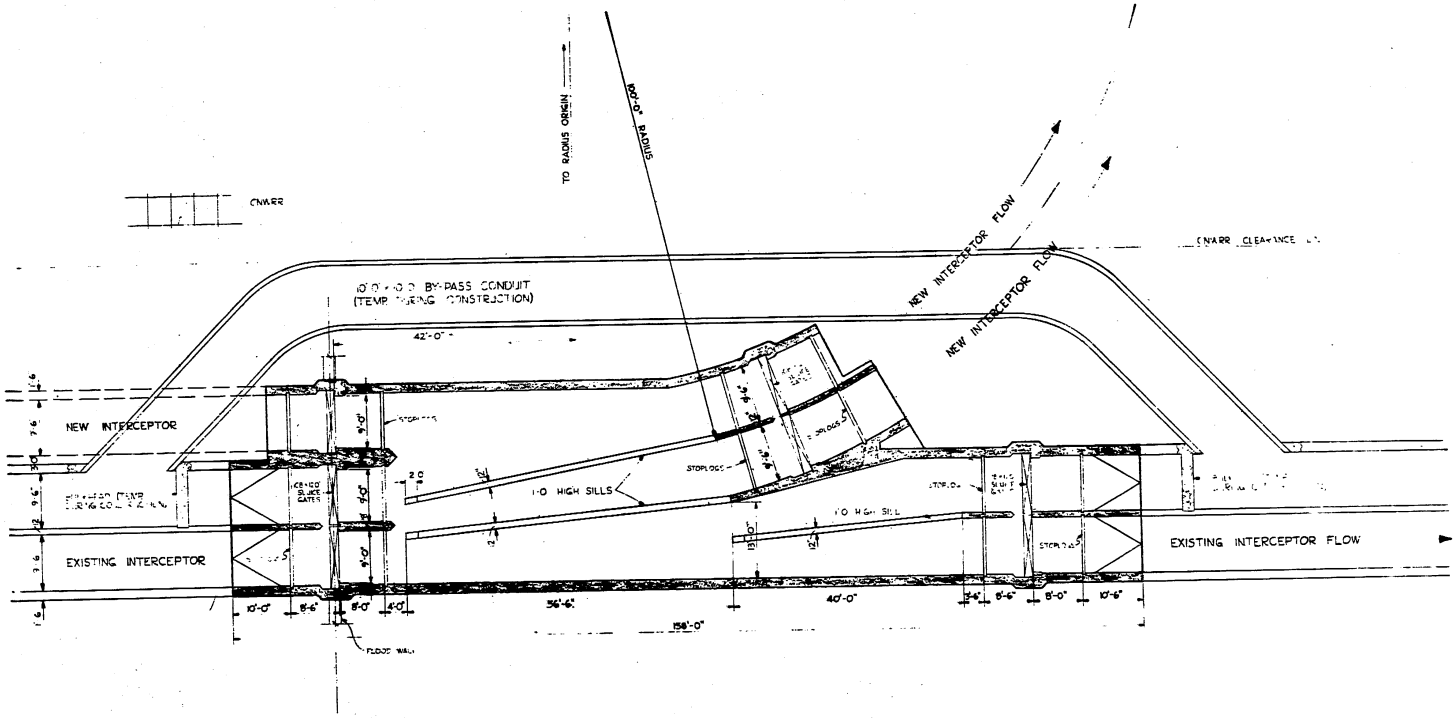

Fig. 1 - Plan View of Diversion Structure as Proposed

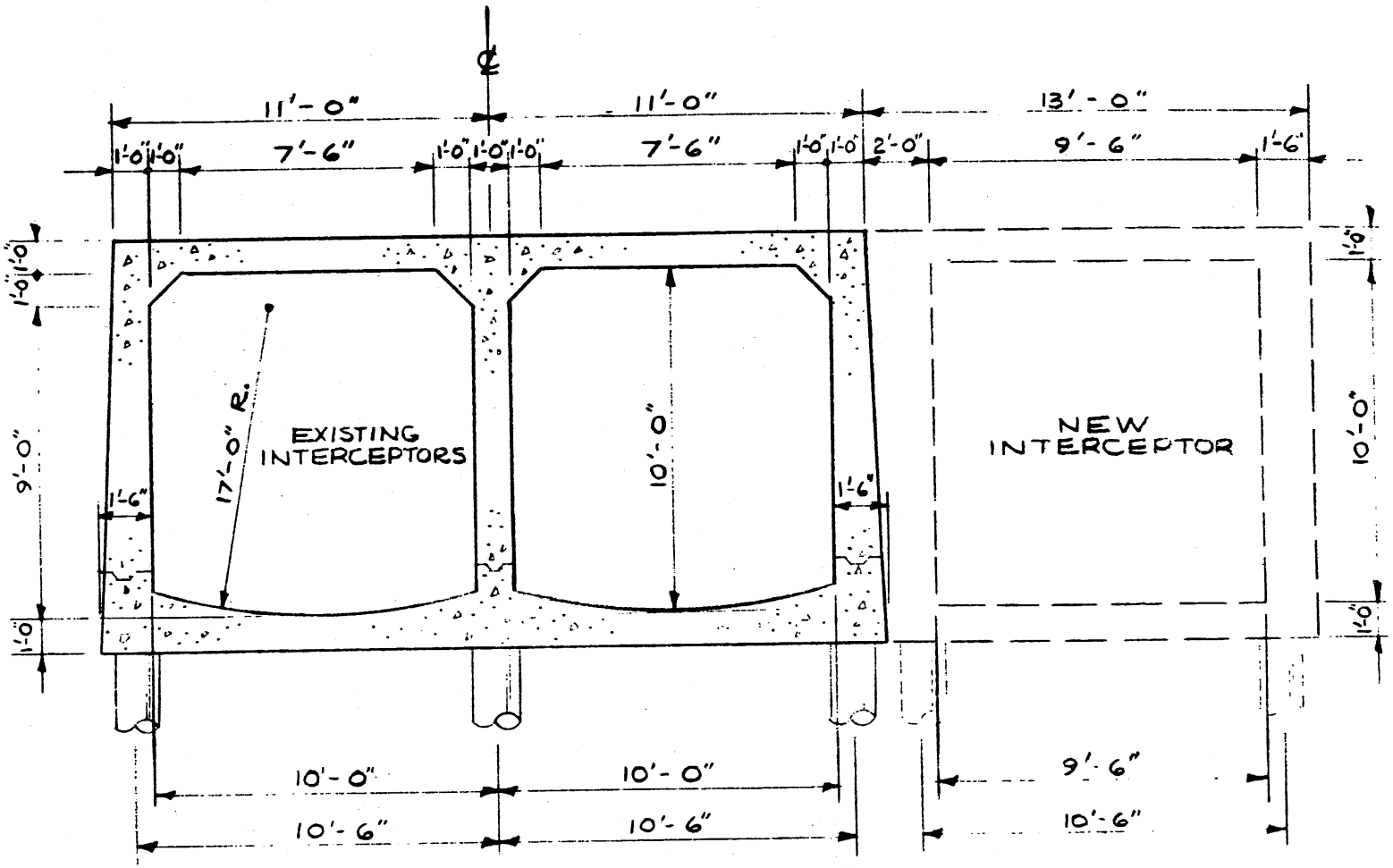

Fig. 2 - Cross section through Existing Combined Main Interceptor looking Upstream

flow depths given in Table A-1. After the diversion structure has been built these depths should still be found at the downstream end of the western (old) branch of the diversion structure, according to the principles of open channel flow, provided that the diversion structure does not change the flow regime from subcritical to supercritical. Flow depths in the physical model will be controlled to give these specified depths at the downstream end of the diversion structure.

Typical grain-size distributions for grit are given in Fig. 3. They are from a previous model study of the grit chambers [2] and an ASCE manual [3]. Size distributions obviously vary widely, presumably depending on a number of factors such as surface cover of the watershed and maximum flow in the sewer preceding the sampling.

According to the critical tractive force concept, a solid particle will be moved along the bed if a critical tractive shear stress is exceeded. Critical tractive shear stresses (after Shields) depend on grain size. An approximate relationship for the critical tractive force [4] is

$$\tau_c = 0.06(\gamma_s - \gamma)d_s = 6.18\ d_s \qquad (1)$$

Typical values of τ_c are

Grit Particle Size d (mm)	Critical Tractive Force τ_c (lbs/sq ft) Average	Range
5	.10	(.10)
2	.04	(.025 to .053)
1	.02	(.012 to .032)
0.6	.013	(.007 to .024)
0.2	.004	(.0034 to .018)

Comparison of the above critical shear stresses with shear stresses actually found in the combined main interceptor as shown in Table A-2 provides information on

a. The largest grit particle which will actually be moved at a specified flow rate

b. For smaller grit particles, the amount of shear stress by which the actual shear stress exceeds the critical tractive shear stress. This information is summarized in Table A-3 of Appendix A.

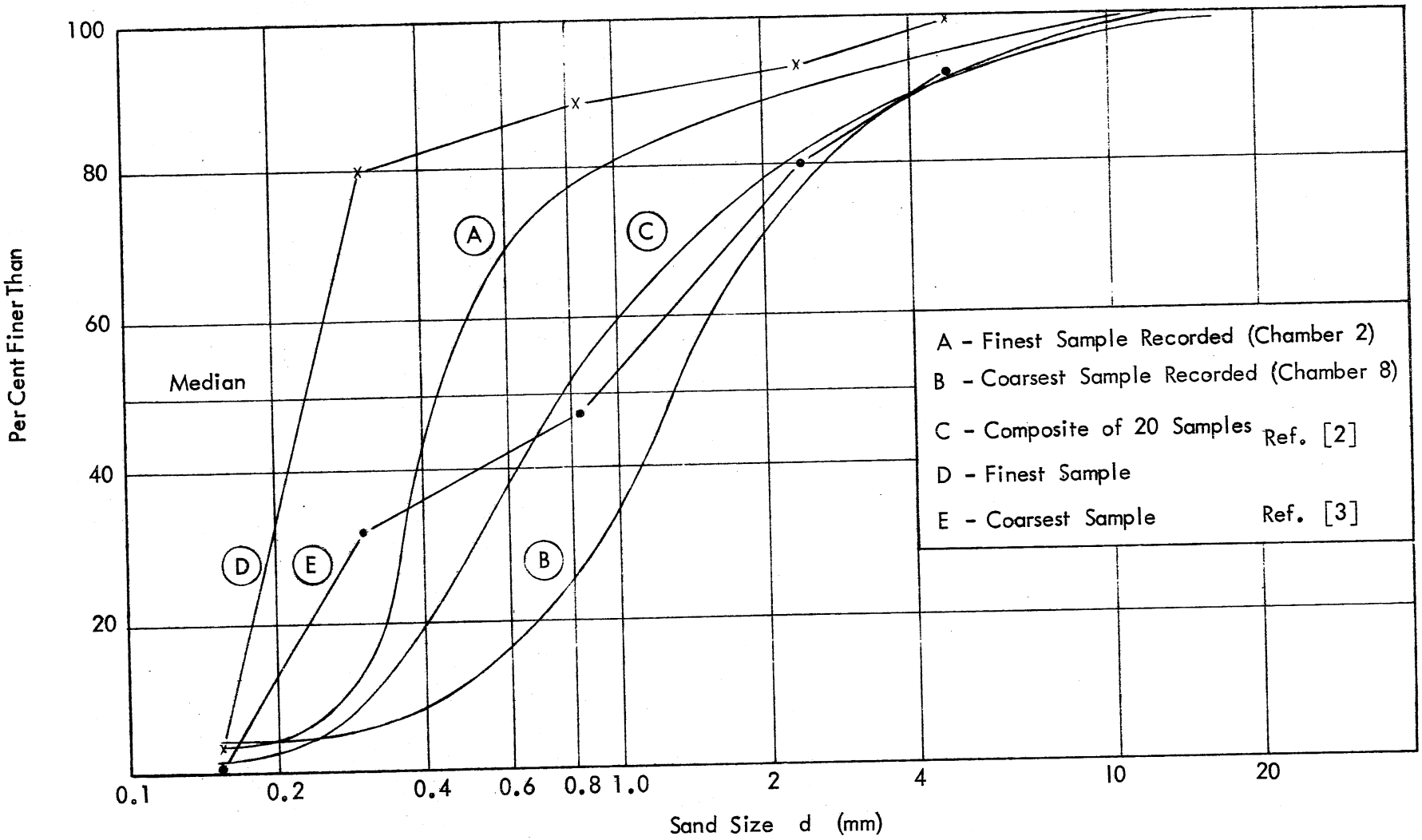

Fig. 3 - Typical Size Distributions for Prototype Grit

Particles smaller than 0.15 mm are usually not removed in the grit chambers, which means that they remain in suspension while the flow goes through the grit chambers. Such particles would also be in suspension in the main interceptor. Particles above a size of 0.15 mm, such as are found in the grit chamber, are usually transported along or near the bed in the main interceptor and in the diversion structure.

The imbalance between grit and water flow through a sewer diversion structure has been studied by Yoshimi and Stelson [5] for the Pittsburgh Sewage Treatment Plant. The study was undertaken because it was noted that the branch channels (outside channels) received 82 per cent of the grit with a passage of only 50 per cent of the water. The geometry of the Pittsburgh diversion structure is considerably different from that projected for the Pig's Eye plant (i.e., the main sewer slopes upward before arriving at the bifurcation), and thus the quantitative results from Ref. [5] cannot be applied. However, some general comments regarding the methods used to reduce the percentage of bed load drawn into the branch channel can provide guidance with regard to the Pig's Eye project. It should be pointed out that the objective of the study described herein is to route a substantial amount of grit into the branch channel because the new grit removal system will be more efficient than the old one. This objective is the opposite of that of the study described in Ref. [5].

It is remarked in Ref. [5] that the sanitary engineering literature contains no writing on the subject of grit diversion. Since that paper was written Silberman and Paintal [2] have carried out a study of grit distribution for the existing Pig's Eye treatment plant.

The hydromechanics of grit and water diversion in a branching interceptor system are very similar to those which must be considered in the designing of branching alluvial canal systems, water diversion structures, and river regulation. It is therefore possible to extract some information from publications such as Refs. [6] through [10].

The reason water and grit (bed load) do not flow in the same proportion into the branch and the main channel of a channel bifurcation is stated in Ref. [5] in the following way:

> In order to obtain flow in a branch channel, at least the direction if not the magnitude (speed) of the velocity vector must be changed. Then a change in momentum results.

> Because the water near the bottom that transports the bed load flows more slowly than the upper layers, it possesses less forward momentum and is more readily subject to changes in momentum. Therefore it is more readily diverted into the branch channel together with the bed load. Experiments have shown that, in the case of a rectangular branch channel transporting 50 per cent of the total flow, a major portion of the bed load (at least 80 per cent) may be drawn into the branch regardless of the angle of divergence [Ref. 10 herein].

The lower fluid layers, which possess less velocity, are turned more easily and more quickly than the upper layers when the water moves around a curve. The result is secondary motion in spiral form which tends to turn the lower water along with the bed load toward the convex side of the curve.

Reference [5] also points out correctly that "a number of methods of bed load deviation have been successful when total exclusion of the bed load from a branch or main canal was intended," and goes on to say that "the requirement of balanced division of grit as is desirable in most treatment plants is a much more difficult achievement." The transverse circulation of water in a channel which is responsible for the bed load transport is explained in more detail in Refs. [7] and [8].

The diversion structure to be investigated for the Pig's Eye treatment plant is not only a channel bifurcation, but also a sudden channel expansion at the upstream end. The transverse circulation patterns are not really predictable. A model study therefore had to be undertaken to study the currents and the bed load transport produced. In this study, modification of the transverse currents is considered the key to a suitable solution regarding grit and water distribution in the channel branches. This is in agreement with the methods described by Mamak [7] for achieving channel shaping.

IV. MODEL DESIGN

The hydraulic (physical) model had to be a gravity flow and bed load transport model and to satisfy simultaneously similarity criteria for free surface flow and sediment transport. Dynamic similarity had to be provided in addition to geometrical similitude so that the phenomena observed in the model and the measurements made in the model would be similar to those found in the prototype.

The forces dominating the hydraulics of the flow through a branching canal are primarily inertial and gravitational forces, while those controlling the grit transport on the bed are primarily shear forces and buoyancy forces. It is therefore appropriate and necessary to choose different similarity criteria for the overall model design and the grit transport. The overall model was designed to satisfy Froude similarity. The grit transport was modeled using a bed shear stress criterion. According to this criterion the actual bed shear stress produced by the turbulent flow in the sewer barrel and the so-called "critical tractive force", the shear stress, which is necessary to set a grit particle in motion must be in the same or at least reasonable proportion in the model and the prototype. A "model grit" must be chosen so that this condition is satisfied.

In addition to these similarity criteria it was necessary to assure that the flow would be turbulent everywhere in the model. It was also necessary to build the model large enough so that secondary currents, which are primarily responsible for the distribution of the grit, would develop in approximately the same way in the model as they do in the prototype. In previous studies of this kind geometrical model scales of 1:12 [2] and 1:8 [5] have been applied. A scale of 1:12 was considered appropriate for this study.

At a 1:12 geometrical scale, Froude similarity requires the following scaling factors (model to prototype) for the flow parameters:

Water depths (ft)	1:12
Areas (sq ft)	1:144
Flow velocities (fps)	1:3.464
Flow rates (cfs)	1:498.8
Pressures (psi)	1:12

With these provisions in mind and the dimensions and flow rates of the prototype given, a model with the following characteristics was designed: a test section 13.2 ft long, including a 90° bend of 8.33 ft radius; an approach channel 14 ft long consisting of three sewer barrels (two in existence, one projected); and one tail channel 6.3 ft long following the southern and eastern branch channels respectively. The geometry of each section was in accordance with the specifications contained in the drawings furnished by Toltz, King, Duvall, Anderson and Associates, Inc., and reproduced in Fig. 1.

An entrance or approach section was required to produce a fully developed flow in terms of the velocity distribution as found in the prototype. A tail section was required in each branch because the flow through the diversion structure is expected to be subcritical. It was therefore necessary to model a short section of the main interceptor downstream from the diversion.

The general model layout is shown in Fig. 4. A longitudinal section and selected cross sections are given in Fig. 5. The test section was built of lucite so that the motion of the grit particles and the currents could be observed at any location and from any angle. This is most desirable when complex three-dimensional flow patterns are to be expected. The approach channel and the tail sections were built of plywood. The bottom profile was filled in with concrete. The headbox and the tailboxes were built of concrete blocks. Two coats of paint were applied to all materials except the lucite. Figures 6 through 9 are photographs of the model after completion. Figure 6 is an overall view of the model. The rim of the head tank and a large screen to dissipate surface waves in the head tank can be noted in the foreground. The approach channel, the diversion structure, the tail sections, and the tailwater tanks can be clearly seen. In the background a movable carriage spans the width of the basin in which the model is installed.

Figure 7 is a close-up of the diversion structure model showing the high degree of transparency of that section of the model. One downstream control gate in the tail section and one tailwater box are also visible.

The model is run with Mississippi River water at rates up to 2.88 cfs. The water supply flows through a 12-inch pipe connected to the laboratory water supply system into a head tank holding approximately 400 cu ft of water. The inflow rate is regulated with the aid of the hydraulically operated gate valve shown in Fig. 9 preceded by an orifice flow meter. A precision U-tube manometer, also shown in Fig. 9, measures the head differential.

Figure 9 shows the diversion structure model and the approach channel looking upstream. The two existing main interceptor barrels are on the left and the proposed expansion is on the right.

The depth of flow in the model is adjusted by means of sluice gates installed in each of the tail channels. These gates are also used to

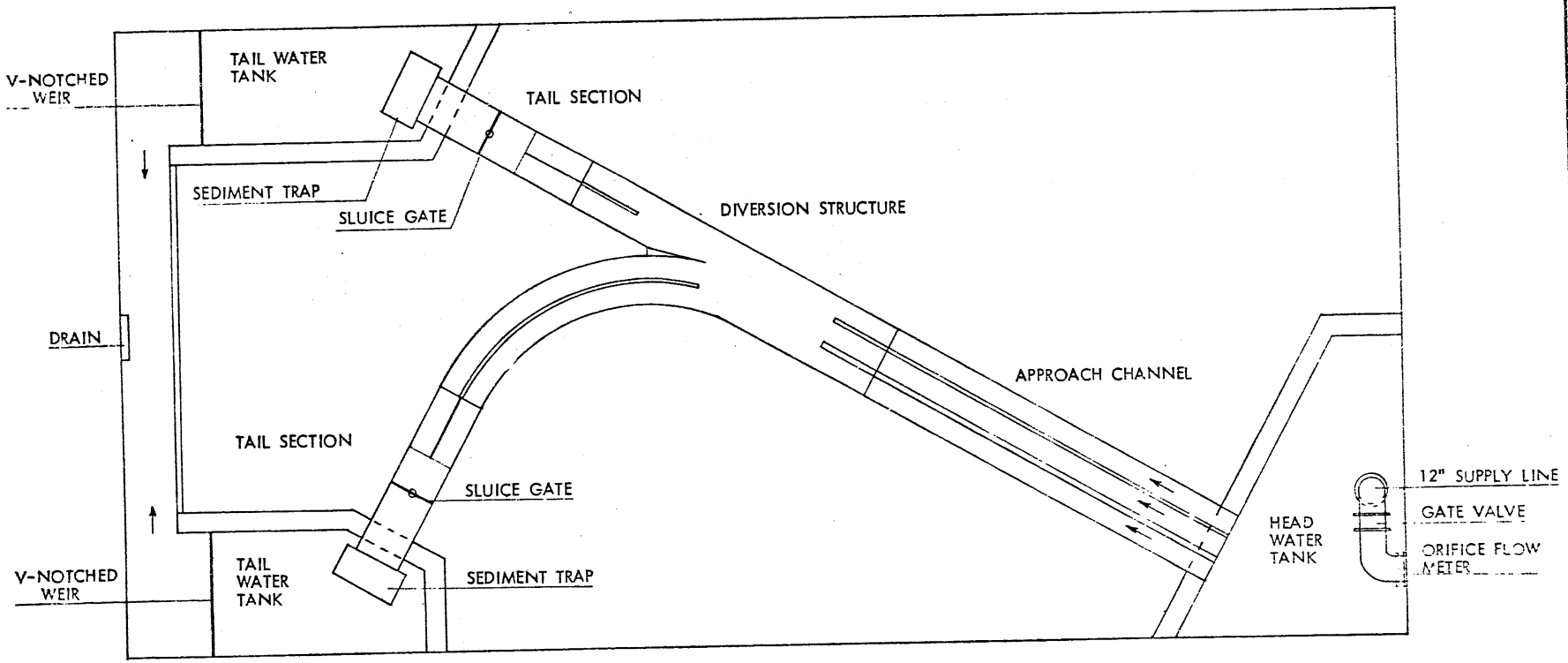

Fig. 4
MAIN INTERCEPTOR DIVERSION
PLAN VIEW OF MODEL LAYOUT

SAINT ANTHONY FALLS HYDRAULIC LABORATORY
UNIVERSITY OF MINNESOTA

DRAWN	CHECKED	APPROVED
SCALE 1:48	DATE	NO.

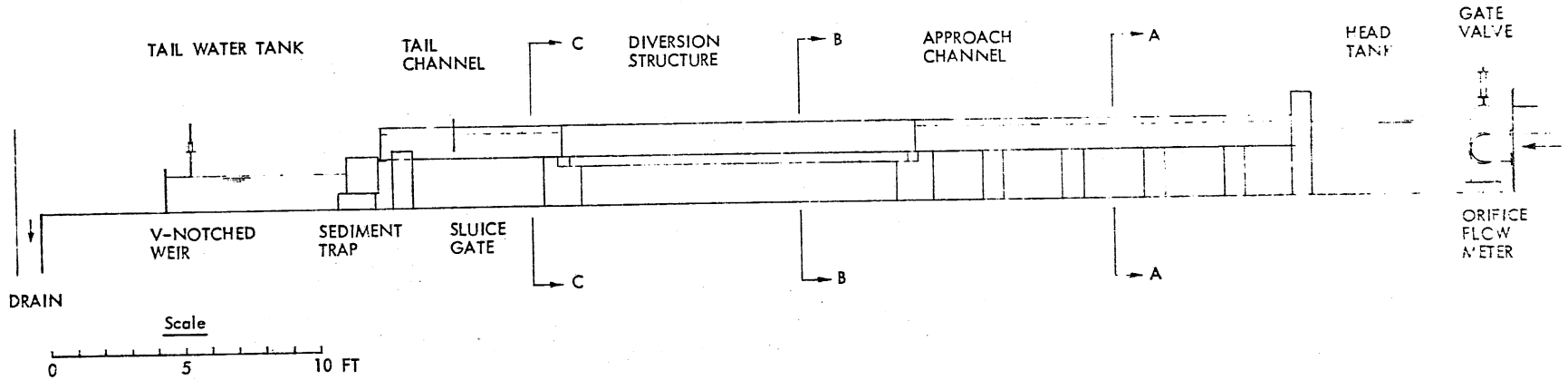

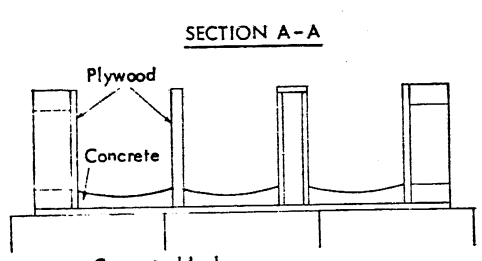

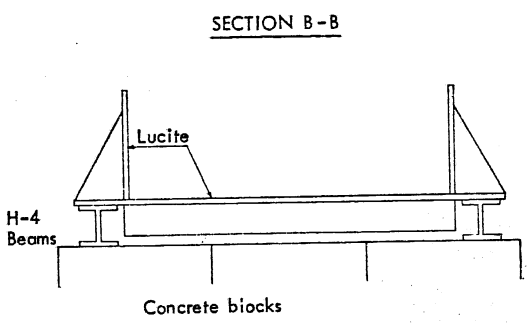

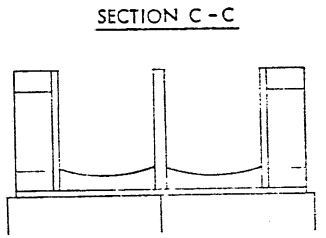

Fig. 5
MAIN INTERCEPTOR DIVERSION
VERTICAL SECTIONS THROUGH MODEL

SAINT ANTHONY FALLS HYDRAULIC LABORATORY
UNIVERSITY OF MINNESOTA

DRAWN	CHECKED	APPROVED
SCALE	DATE	NO

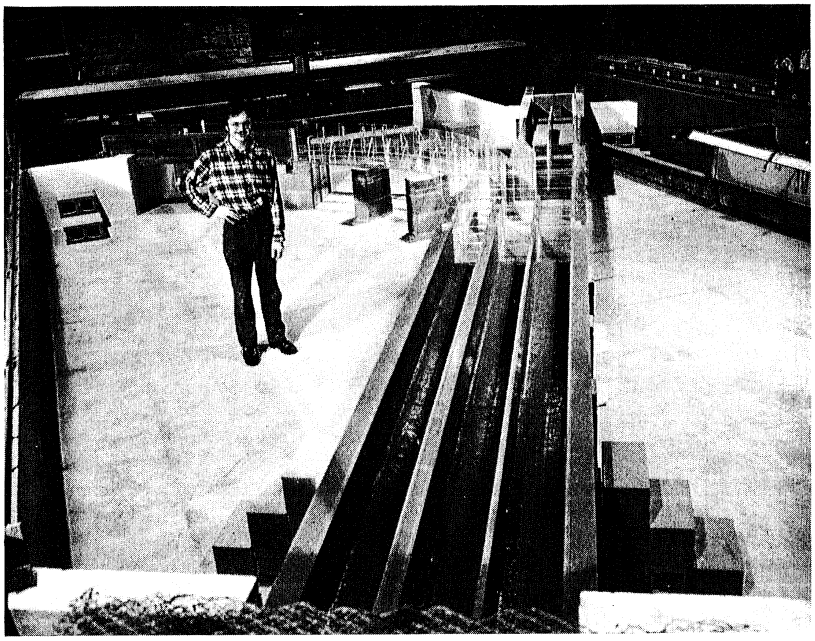

Fig. 6 - Overall View of Model looking Downstream

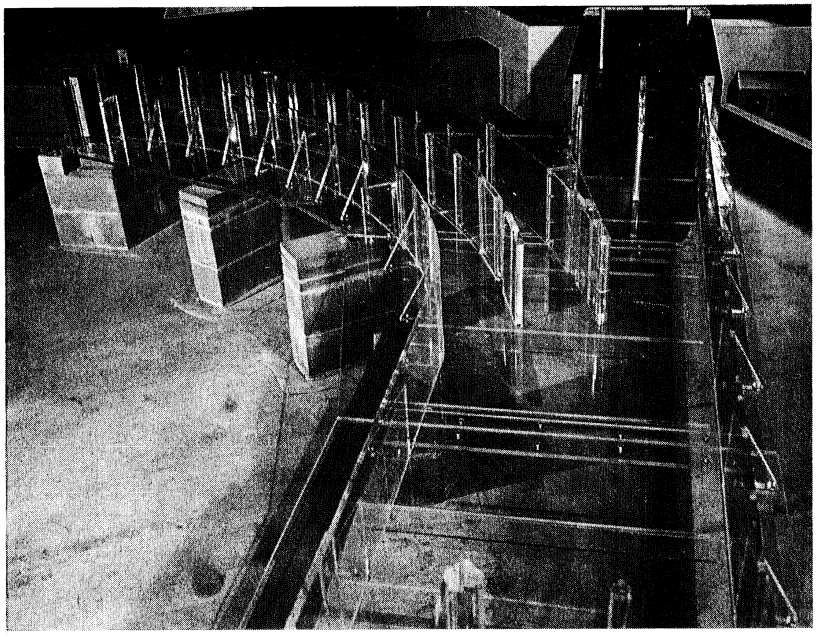

Fig. 7 - Close-up of Diversion Structure looking Downstream along axis of Existing Main Interceptor

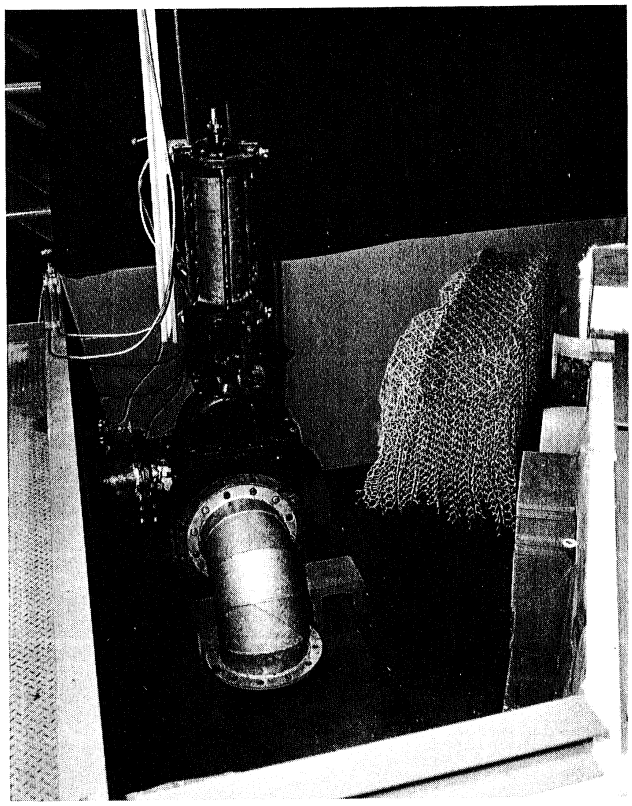

Fig. 8 - Oblique View looking into Nearly Empty Head Tank

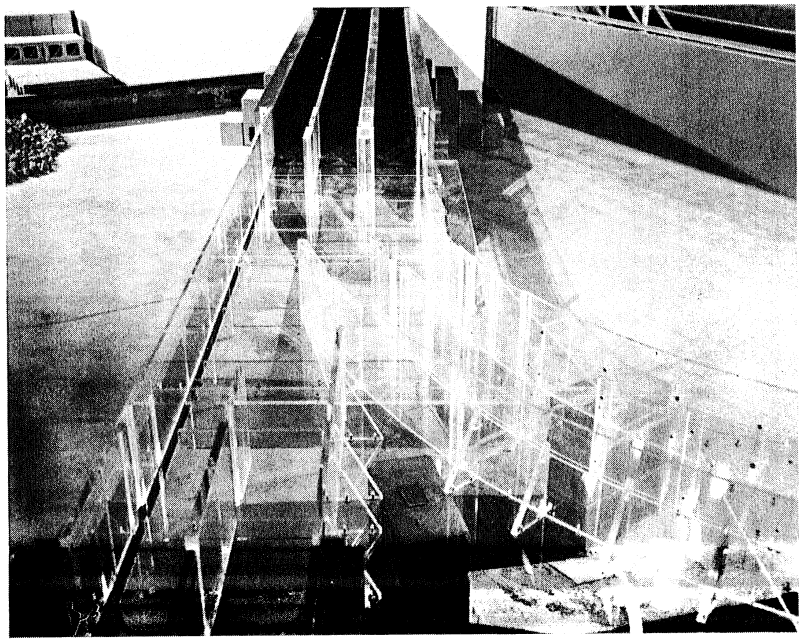

Fig. 9 - Upstream View of Diversion Structure and Approach Channel

achieve the desired flow distribution between the east (new) and the west (old) branch of the interceptor. Each tail section discharges into a tailwater box equipped with a V-notched weir for the flow measurement as shown in Fig. 10. The identical V-notched weirs, as well as the orifice meter in the headbox, were calibrated experimentally prior to operation. A point gage is installed in each tailwater box and on the movable carriage covering the model area.

A grit trap is installed at the end of each tail section. The grit traps are essentially galvanized sheet metal boxes covered by lids and having screened walls. When the lid is opened, the flow is diverted into and through the box. The grit is retained in the box while the water passes through. The installation can be seen in Fig. 10.

Figure 11 shows the full extent of the lucite diversion structure model as originally projected, but without sills.

The required hydraulic characteristics of the model were obtained by applying the previously quoted scale ratios to the values given in Tables A-1 and A-2. The results are given in Appendix B, Table B-1.

While perfect similarity of depths and pressures can be achieved at a scale ratio of 1:12, bed shear stresses will be reduced by a factor only approximately equal to 12. (This stems from the well-known fact that Froude similarity and Reynolds similarity cannot be achieved simultaneously in an undistorted model.) It is informative to calculate the average bed shear stress which will be obtained in the model and compare it to that of the prototype. The pertinent figures have been assembled in Appendix B, Table B-1. Hydraulically smooth surface conditions have been assumed for the model.

Four types of model grit were selected for use at different flow rates. They were chosen so that the model grit would be moved slowly along the bed of the approach channel at the flow rate under investigation. Upon entering the section the particles move along those flow paths where high bed shear stresses are sustained, but are deposited where the bed shear stresses are low. This will also occur in the prototype. The grain size distributions and specific gravities of the selected model grits are shown in Fig. 12.

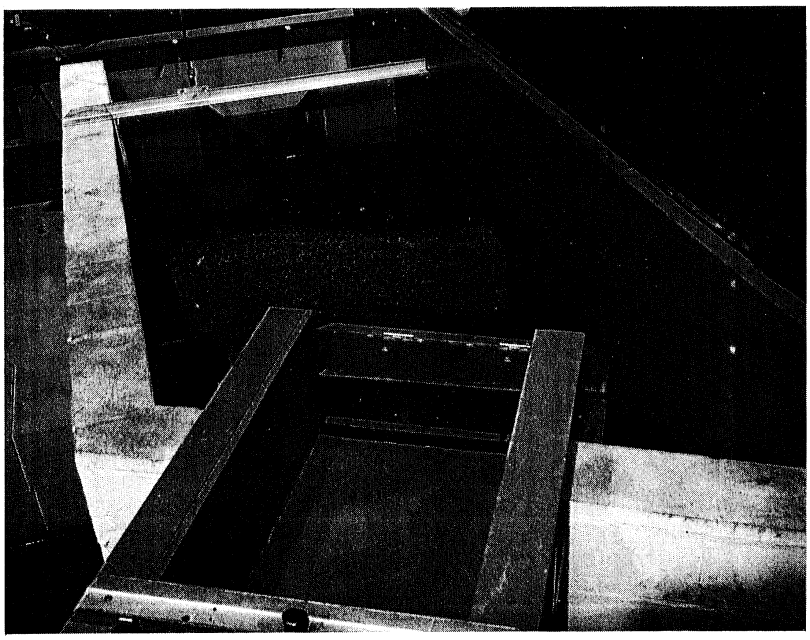

Fig. 10 - View looking into the Nearly Empty Tailwater Tank

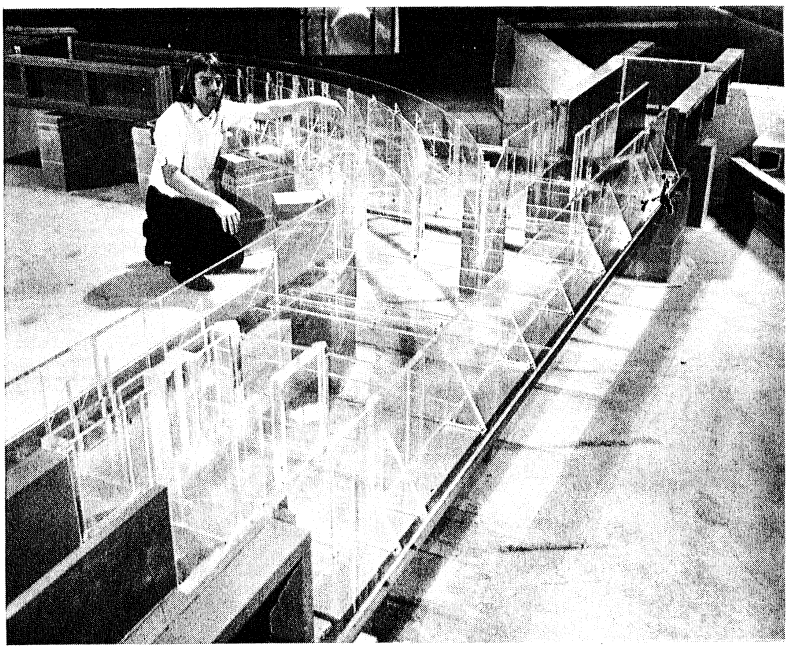

Fig. 11 - Full View of the Lucite Diversion Structure Model

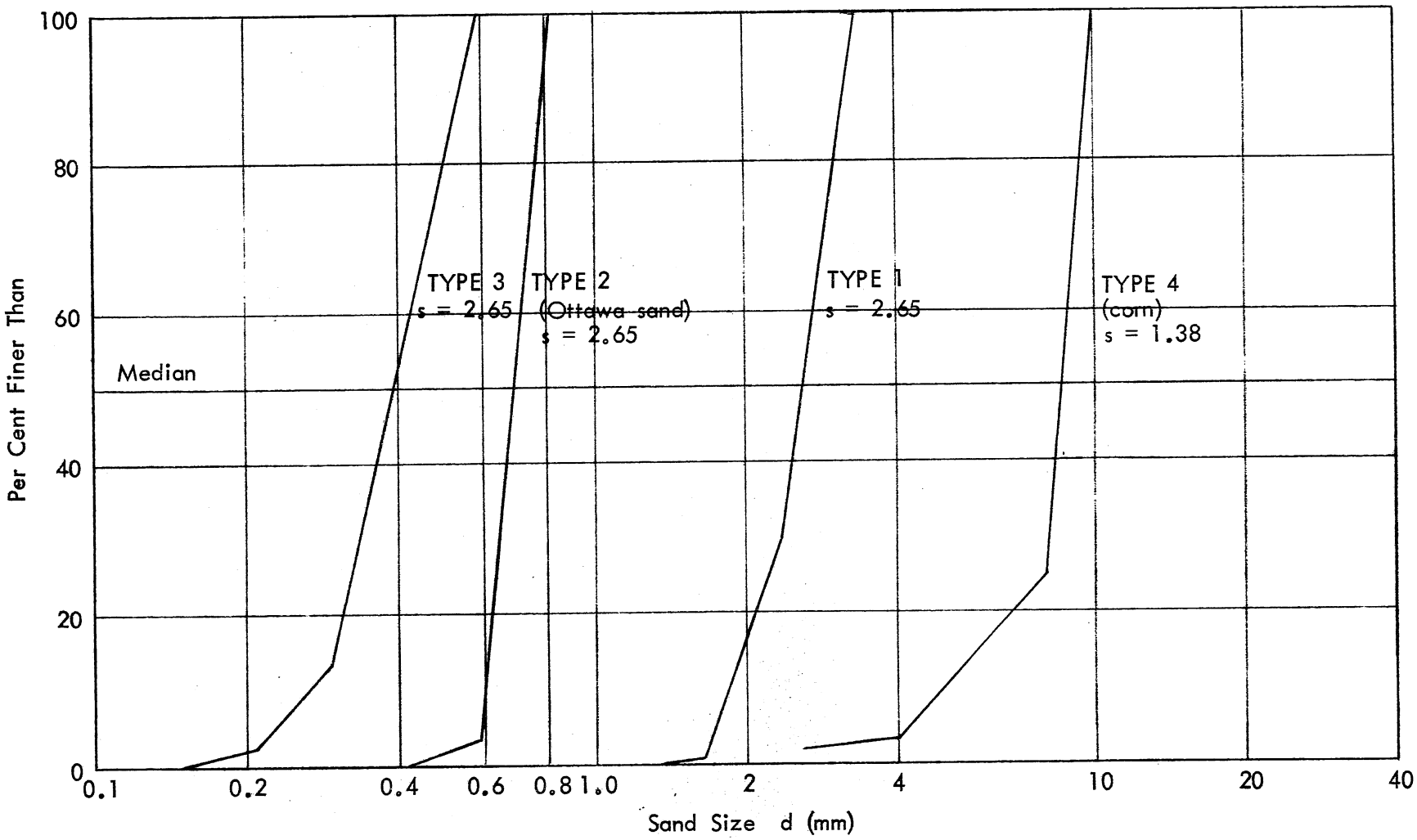

Fig. 12 - Model Grit Size Distributions

The model grit chosen is larger than geometrical similarity requires because very fine particles (less than 0.1 mm) are difficult to disperse in water and difficult to sample. However, the model grit is small enough to be transported by the model flow along the bed of the model main interceptor. The model grit represents essentially the coarser fraction of the prototype grit (which moves along the bed). It can be expected that the model grit will move along the same paths and form the same deposition patterns as the coarse prototype grit.

The finer fraction of the prototype grit cannot be adequately represented in the model. However, this is not a serious deficiency, because the finest fraction of the grit can be expected to be moved in suspension rather than on the bed and is therefore more likely to be divided in the same proportions as the water. The high values of shear stress ratio shown in the last line of Table A-3 support the concept of suspended motion for the fine grit particles.

More information on suspended sediment transport can be found in Refs. [4], [11], and [12].

V. EXPERIMENTAL PROCEDURES

The following basic information was obtained and recorded:

a. Water depths (water surface profiles) along all walls of the test section. These were usually recorded before and after grit deposition.

b. Deposition patterns of grit in the diversion structure. These were recorded photographically and by measuring bed profiles in selected cross sections with a point gage from a carriage.

c. Grit loads in the east and west branches of the combined main interceptor through the use of the sediment traps.

The test procedure most frequently applied is as follows:

1. After the model has been cleared of deposits from previous experiments, the desired total flow through the model is established using the main control valve at the upstream end.

2. The sluice gates in the two tail sections are set to provide (a) the desired water depth in the west (old) interceptor downstream from the diversion structure and (b) the desired distribution of sewage flows in the two branches. This requires some trial and error and use of the V-notched weirs.
3. Water surface profiles are recorded.
4. Grit is added in the approach at a uniform rate and deposits are gradually built up.
5. When a steady-state bed configuration has developed, the grit traps are opened for a period of time.
6. The volumetric proportions of grit accumulated in each trap are measured using a graduated cylinder.
7. Water surface profiles are recorded.
8. Flow through the model is stopped and the residual water drained carefully.
9. Photographs of the bed configurations are taken from two different angles.
10. Measurements of selected bed profiles are obtained.

Stations at which bed profiles or flow depths were measured in the model are shown in Fig. 13.

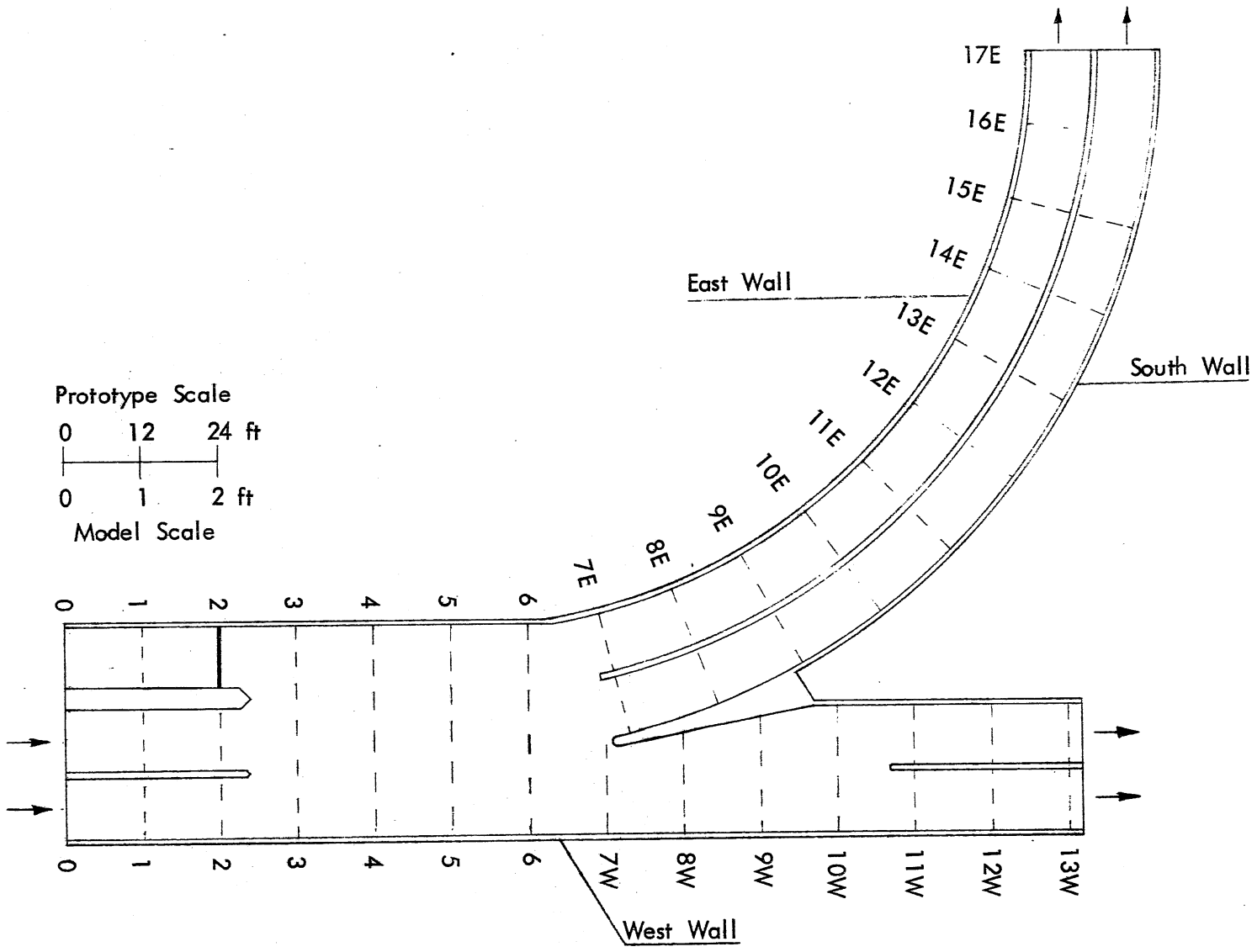

Fig. 13 - Stations (cross sections) at which Bed Profiles were measured

Although experience shows that a rigidly defined test sequence for a study with unpredictable results is not very useful, it is nevertheless necessary to make a tentative plan. Such a plan was followed with some modifications, resulting in the following series of experiments:

SERIES I: Experiments for flows of 620 mgd with the structural design as proposed, but without any sills on the bottom. The purpose of this series was to study the "unmodified" hydraulics and secondary currents and their effects.

SERIES II: Experiments essentially the same as in Series I, but with sills added as in the original design.

SERIES III: Experiments for alternative structural modifications leading to the proposed design.

SERIES IV: Expanded series of experiments for proposed design; flows of 490, 273, and 176 mgd.

SERIES V: Experiments with three barrels of main interceptor, flow of 930 mgd.

SERIES VI: Experiments with two of the four downstream barrels closed to prevent possible grit deposition in the barrels.

A detailed listing of all experimentally investigated conditions is given in Appendix C, Table C-1.

VI. RESULTS

1. Flow and Grit Transport through Original Structure

Series I: Without Sills

Tests for Series I were run without sills installed on the bed. Flows equivalent to 620 mgd and two types of grit were used.

The hydraulic flow characteristics were found to be rather unsatisfactory. Flow depths varied considerably throughout the diversion structure. To achieve the desired flow distribution, depths of flow in the new (east) branch had to be 4.9 ft, while those in the west (existing) interceptor were 6.5 ft. As a consequence, the water elevations in the new treatment facilities (settling chambers) would need to be lowered accordingly. Water surface elevations measured along the walls of the diversion structure are shown in Fig. I-1. After grit has been deposited in the east channel, water depths appear to be even more different in the two branches of the main interceptor, as shown in Figs. I-2 and I-3.

The flow through the diversion structure is most adequately described as very similar to an undular hydraulic jump. The sudden expansion from the existing main interceptor into the diversion structure causes an acceleration of the water in the last part of the barrel to nearly critical flow conditions. Figure I-1 shows a decrease in flow depth from about 6 ft down to 3.9 ft. At 620 mgd the critical depth of flow in the main interceptor is 2.9 ft. Hence the flow out of the interceptor into the main basin of the diversion structure is not far from being a critical flow. From the beginning of the diversion structure on downstream the water surface is very undulated. As the bulk of the water mass flows on straight toward the branching point, the flow depth increases again. However, at the same time a strong transverse gradient in flow depths develops as shown in Figs. I-1, I-2, and I-3. A large eddy is observed near the easterly wall of the diversion structure. Figure I-4 shows differences in water elevations at the beginning of the branching channel. The flow is from right to left in the photo. A very strong current directly in front of the piers is associated with the transverse water surface slope. The irregular waviness of the water surface in the diversion structure is visible in Fig. I-5. Also apparent, although not as clearly, is the substantial difference in flow velocity between the two sides of the channel.

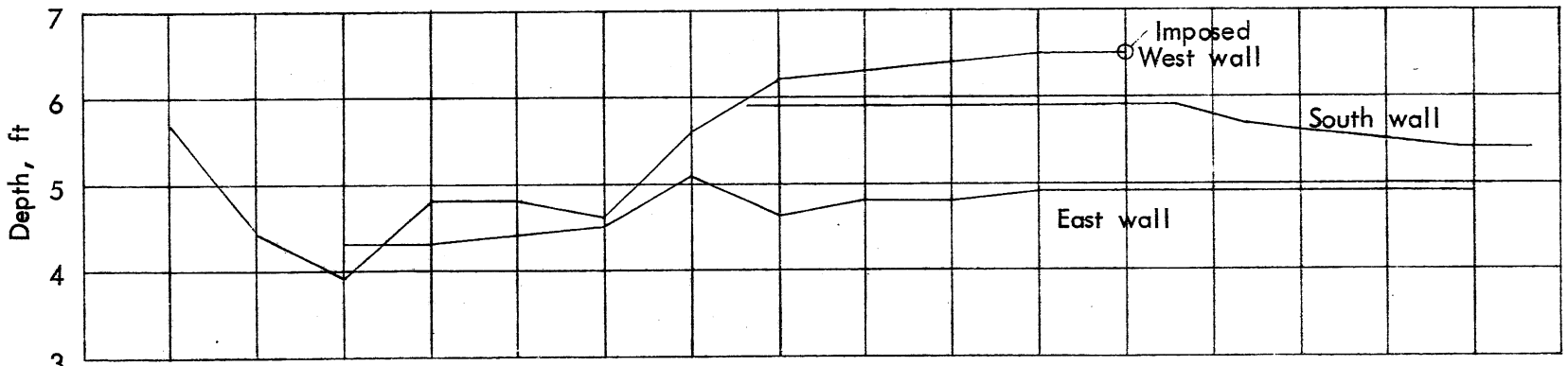

Fig. I-1 - Water Surface Profiles along Walls of Diversion Structure - Exp. 1
620 mgd, 2 mm grit, no sills -- without grit deposit

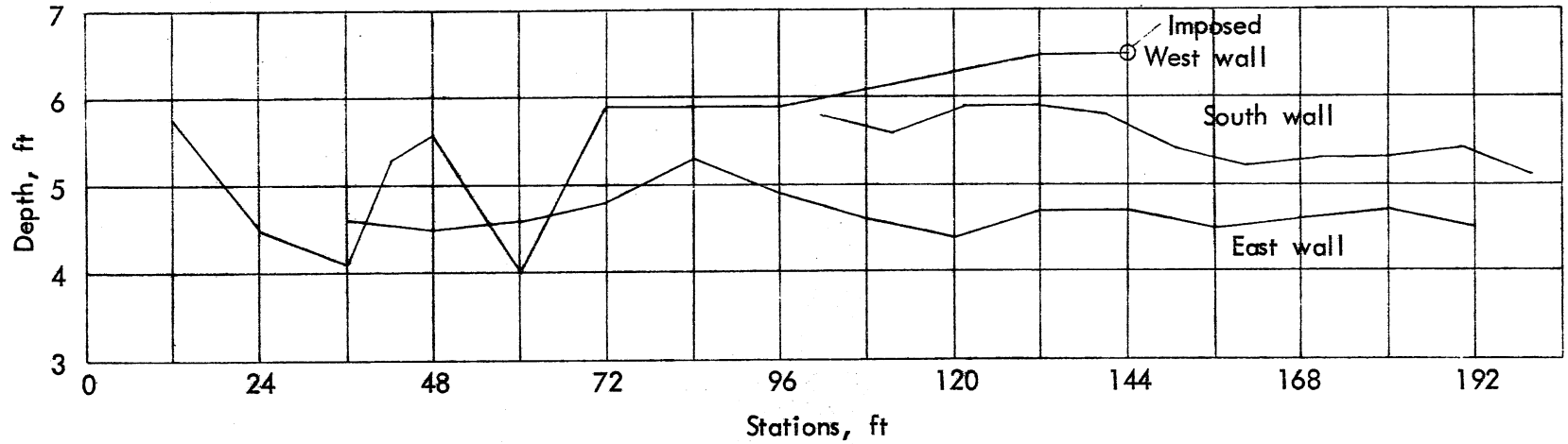

Fig. I-2 - Water Surface Profiles along Walls of Diversion Structure - Exp. 1
620 mgd, 2 mm grit, no sills -- with grit deposit

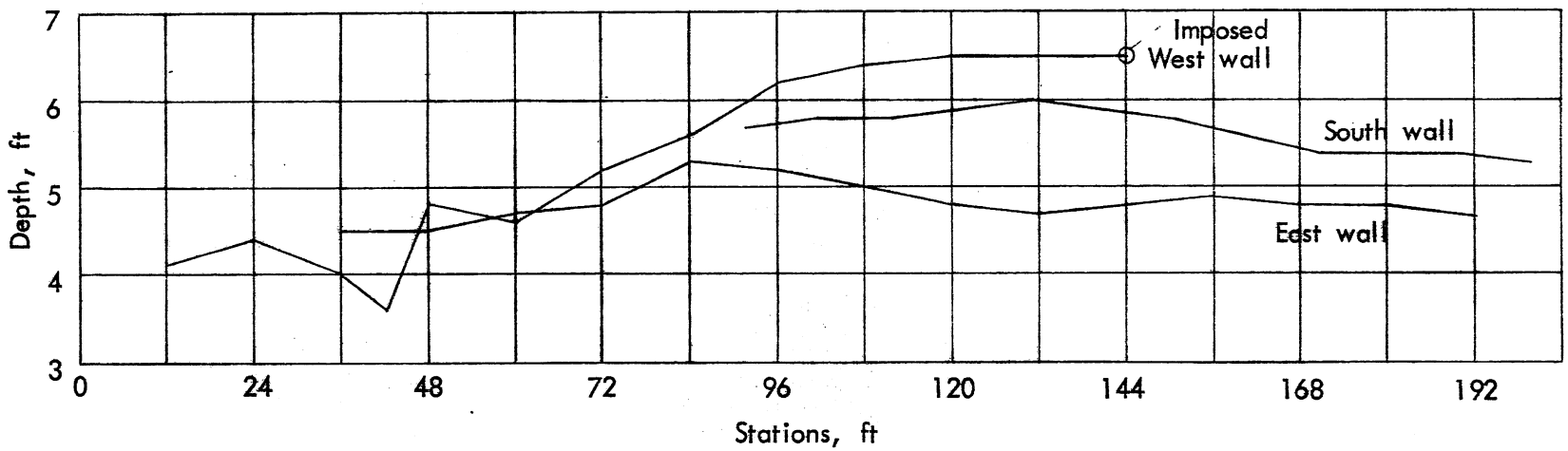

Fig. I-3 - Water Surface Profiles along Walls of Diversion Structure - Exp. 2
620 mgd, 0.7 mm grit, no sills -- with grit deposit

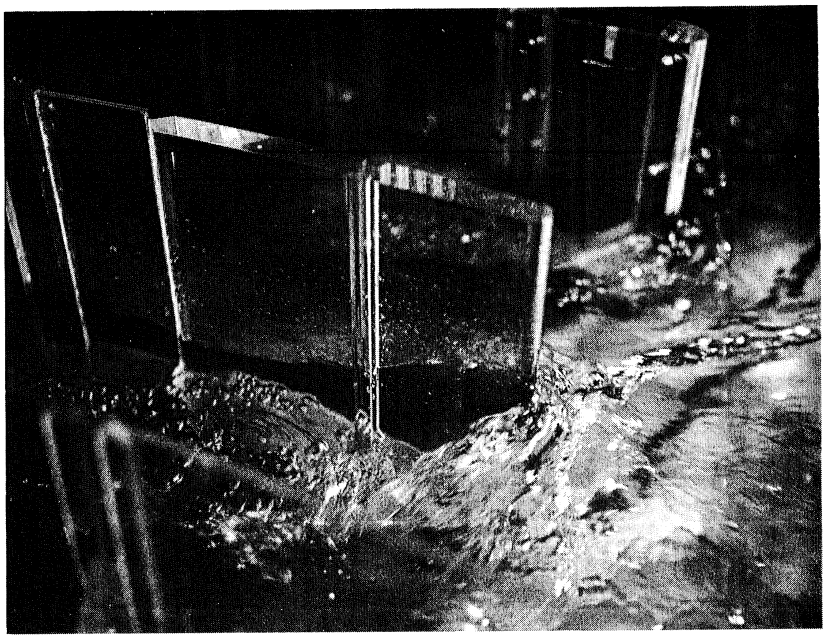

Fig. I-4 - View of Flow Separation Around Piers caused by Strong Transverse Currents at 620 mgd (Series I)

Fig. I-5 - Overhead View of Flow into the Diversion at 620 mgd (Series I)

When grit is added to the flow in the main interceptor (approach channel), most of it will be deposited at one place or another in the diversion structure because of large differentials in local velocities and bed shear stresses. When the experiment and the addition of grit are continued over a period of several hours, eventually a nearly steady state condition is reached such that the shape and volume of the materials deposited no longer change with time. Water surface profiles recorded at that time are reported in Figs. I-2 and I-3 and are somewhat different from those found without grit. Under steady-state conditions it is found that all the grit is carried into the easterly (new) branch, while only a trace (unmeasurable) amount follows the existing interceptor toward the south.

The deposition pattern in the diversion structure is documented in Figs. I-6, I-7, and I-8. The deposition patterns illustrate the direction of the secondary currents along the bed. The deposits in front of the piers are the result of the cross-currents sweeping the bed in front of the piers. It is noteworthy that the material carried into the existing southerly branch is removed from there by a current along the bed almost opposite to the general flow direction. A change in grit size did not seem to affect results very much. The deposits were quite deep locally. Although the depth of the deposit is not directly transposable into the prototype, it was documented by measuring bed profiles at selected cross sections. Figure 13 identifies the locations. Actual measurements are given in Fig. I-9. While the amount of deposit varies with the grit size used in the experiments, the place of deposit and the shape of the deposit do not change appreciably. A finer grit size was used in Experiment 2 than in Experiment 1. The deposit pattern is shown in Fig. I-8, and bed profiles are given in Fig. I-10. Comparison of the results from experiments 1 and 2 shows clearly where the areas of greatest deposition are. It also shows how and by which secondary currents the bed load (grit) is transported. The use of finer grit still resulted in a total grit flow into the east branch of the main interceptor.

A third experiment conducted under Series I used a flow rate of 273 mgd. The smaller flow, associated with smaller velocities, resulted in better hydraulic conditions than were found with the higher flow. Water surface elevations were more uniform, as shown in Fig. I-11. Still, small quantities of grit type 3 (0.4 mm) were totally deflected into the new branch of the main interceptor.

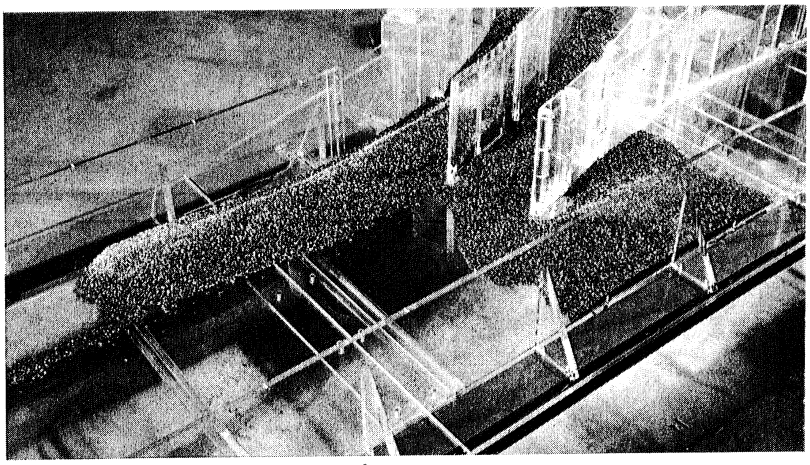

Fig. I-6 - Bed Deposits formed at 620 mgd with Grit Type 1 (Series I)

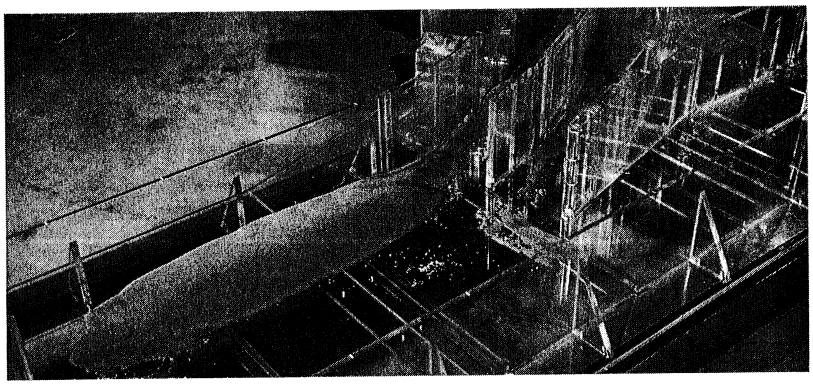

Fig. I-7 - Bed Deposits formed at 620 mgd with Grit Type 2 (Series I)

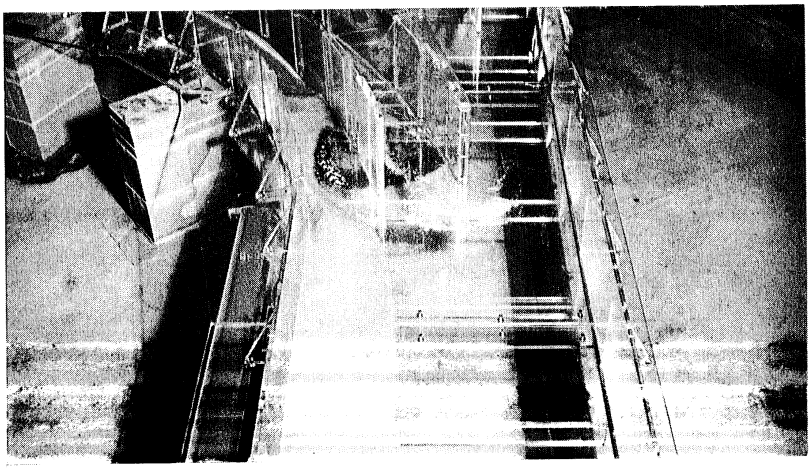

Fig. I-8 - Bed Deposits formed at 620 mgd with Grit Type 2 (Series I)

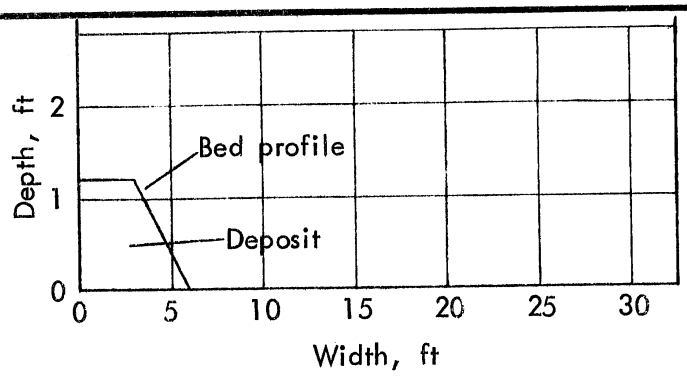

STATION 4

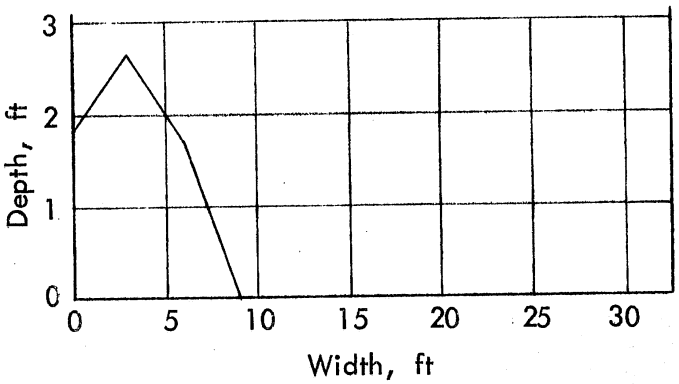

STATION 5

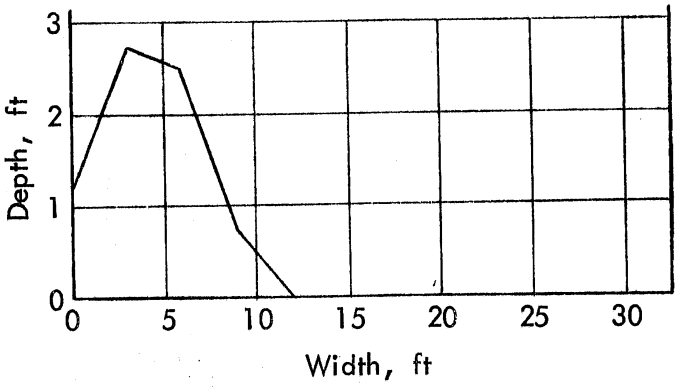

STATION 6

Fig. I- 9 - Bed Profiles of Grit Deposit - Exp. 1
620 mgd, 2 mm grit, no sills

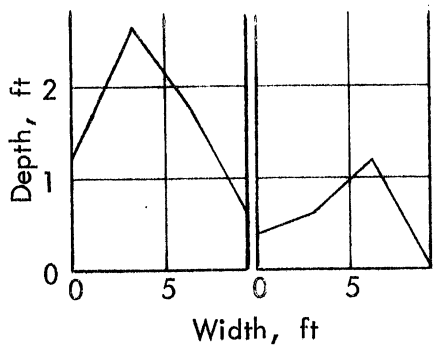

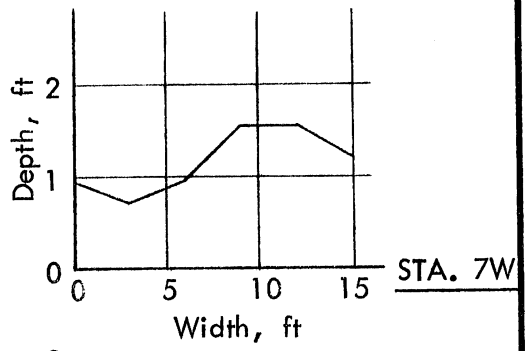

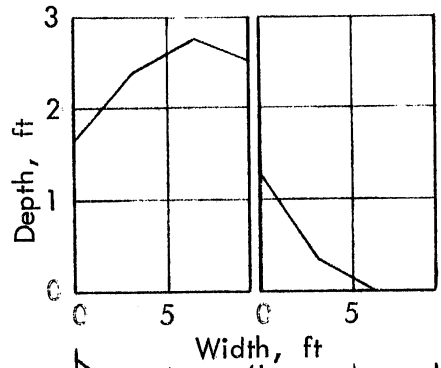

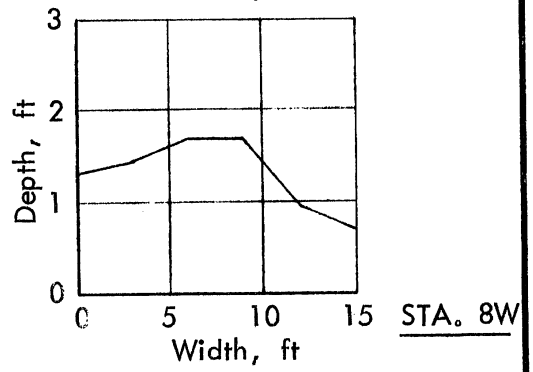

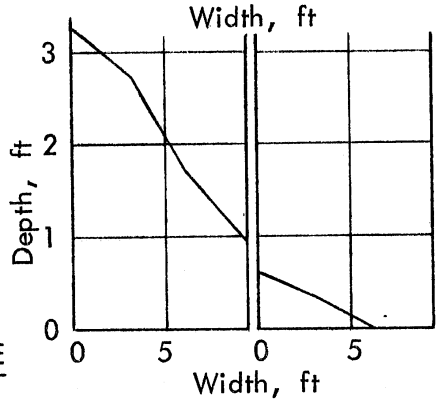

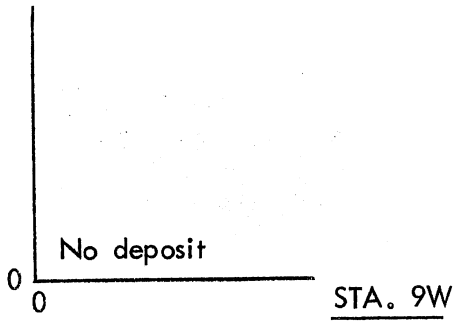

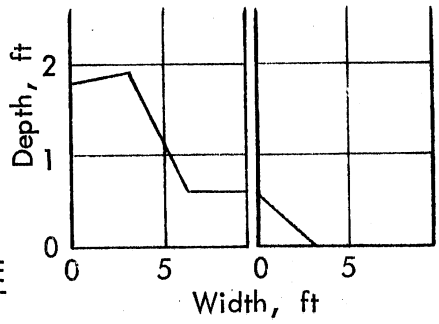

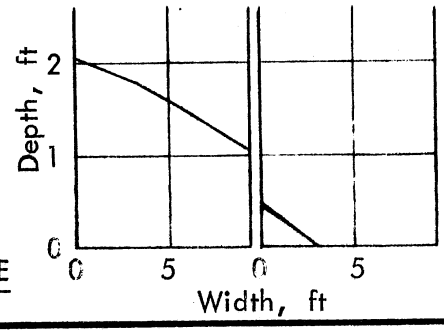

Fig. I-9 (Cont.) - Bed Profiles of Grit Deposit - Exp. 1 620 mgd, 2 mm grit, No sills

STATION 3

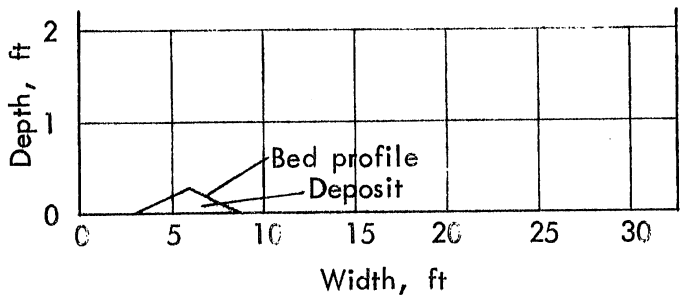

STATION 4

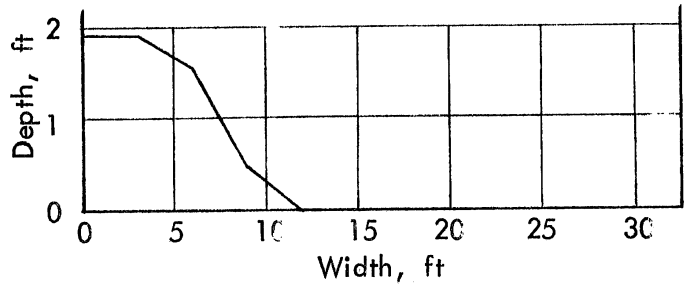

STATION 5

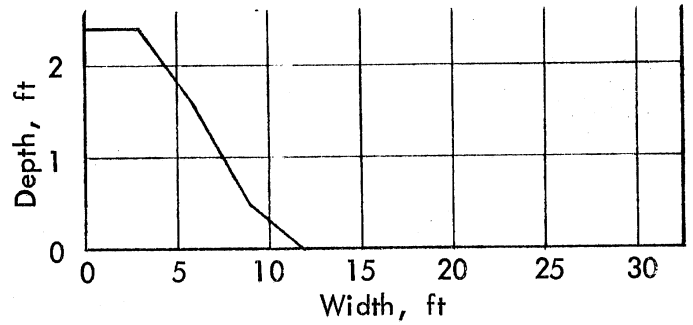

STATION 6

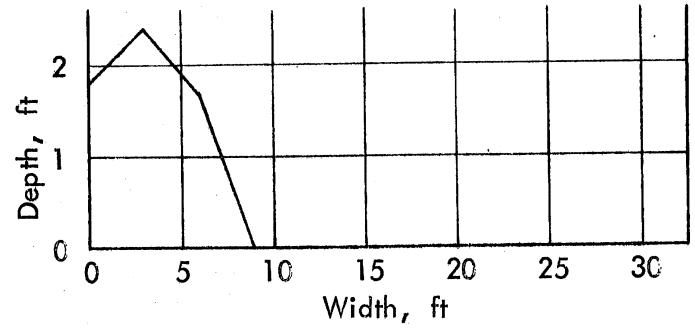

Fig. I-10 - Bed Profiles of Grit Deposit - Exp. 2
620 mgd, 0.7 mm grit, no sills

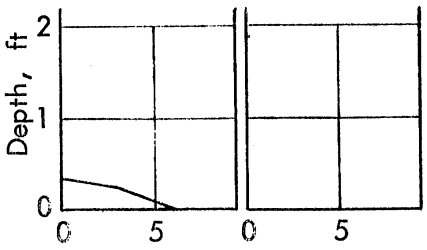

STATION 7E

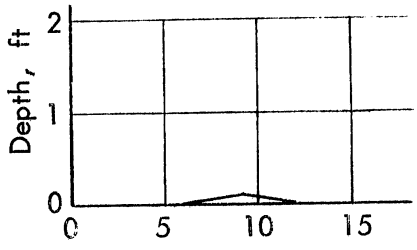

STA. 7W

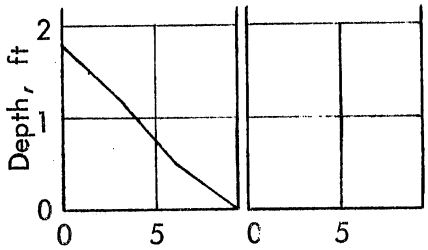

STATION 9E

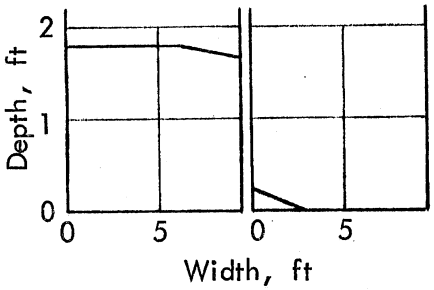

STATION 11E

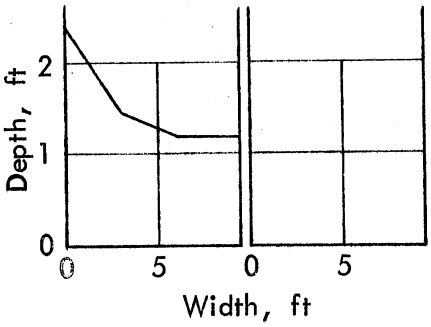

STATION 13E

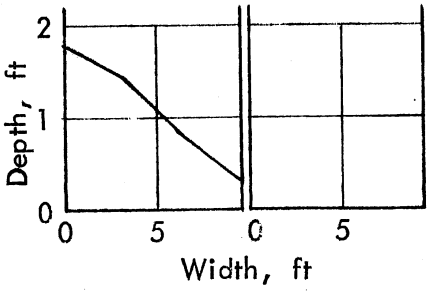

STATION 15E

Fig. I-10 (Cont.) - Bed Profiles of Grit Deposit - Exp. 2
620 mgd,
0.7 mm grit,
No sills

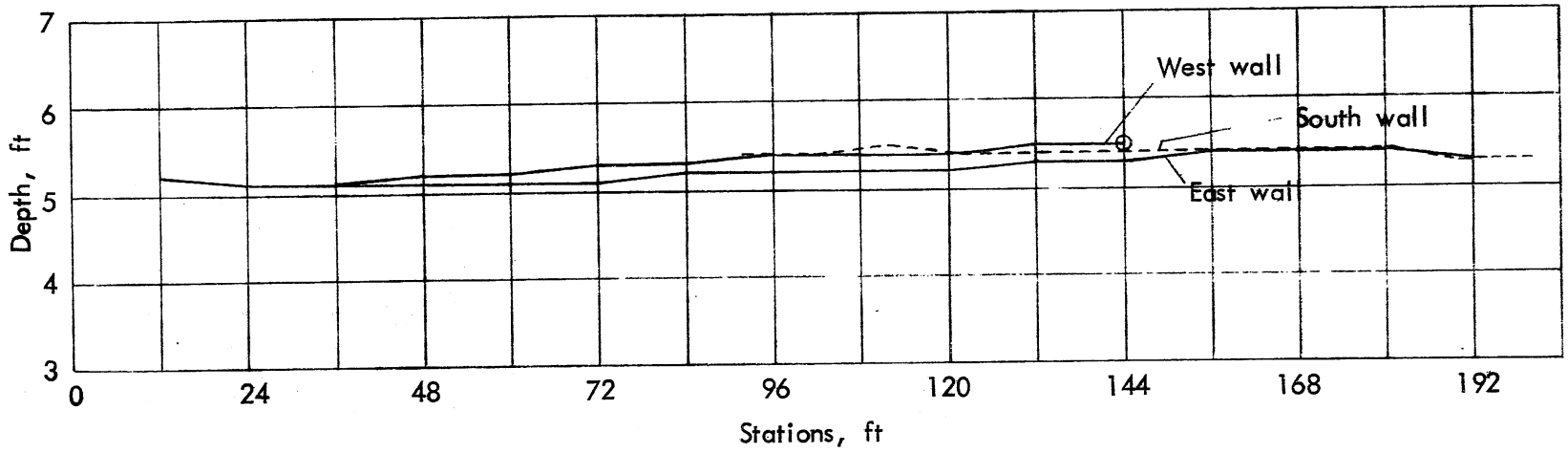

Fig. I-11 - Water Surface Profiles along Walls of Diversion Structure - Exp. 3
272 mgd, no grit, no sills

Series II: With Sills

To determine the effect of sills on flow patterns and grit transport, Experiment No. 1 was essentially repeated, but sills 1 ft high and 1 ft wide were placed on the bed as shown in Fig. 1. The results were again unsatisfactory. It was found in particular that the sills did not substantially affect the total flow or the grit transport rates. Nearly all the grit was still found to go toward the new treatment facilities and almost none toward the existing ones. The grit deposit pattern, shown in Fig. II-1, illustrates how the grit was able, after some deposition, to "jump" the sills. The hydraulics were not much improved. There was still a strong transverse water surface slope in front of the piers, as illustrated in Fig. II-2, and associated with it a strong transverse flow quite similar to the one found in the first series of experiments. Bed profile measurements are given in Fig. II-3.

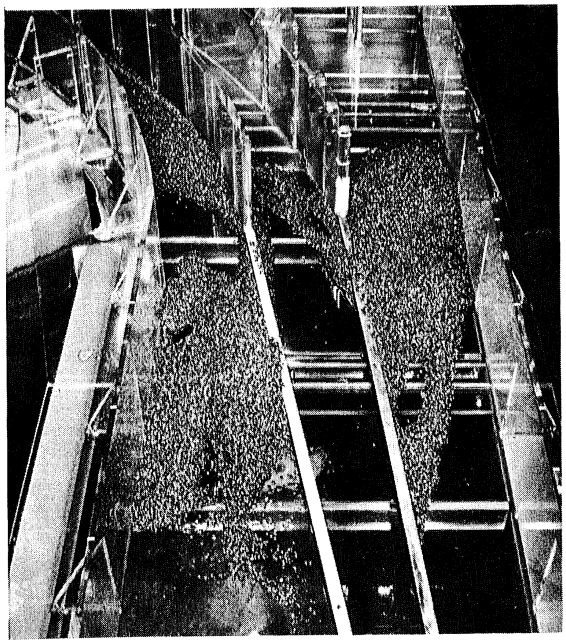

Fig. II-1 - Bed Deposits formed at 620 mgd with Grit Type 1 (Series II)

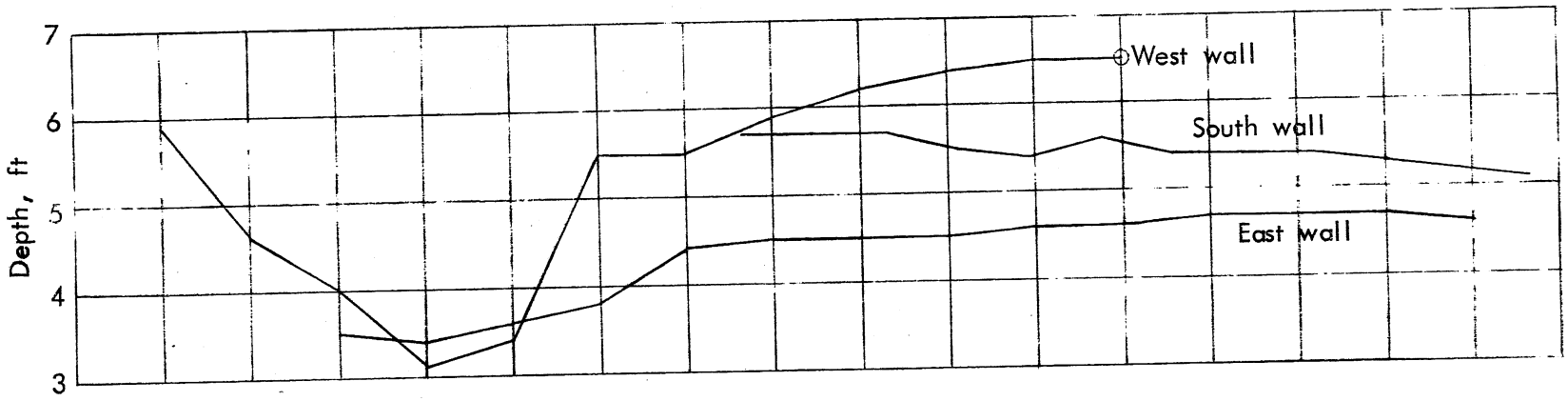

Fig. II-2 - Water Surface Profiles along Walls of Diversion Structure - Exp. 4
620 mgd, 2 mm grit, 1' x 1' sills as shown in Fig. 1 -- without grit deposit

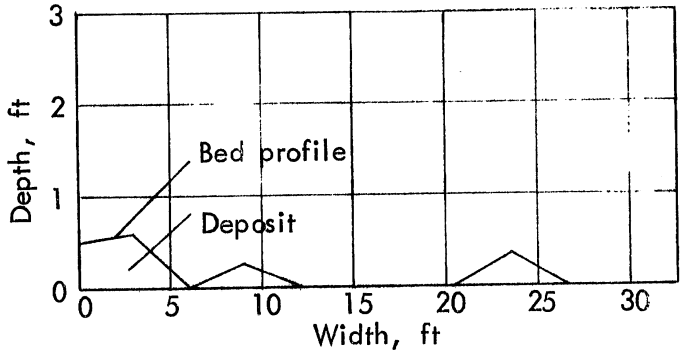

STATION 4

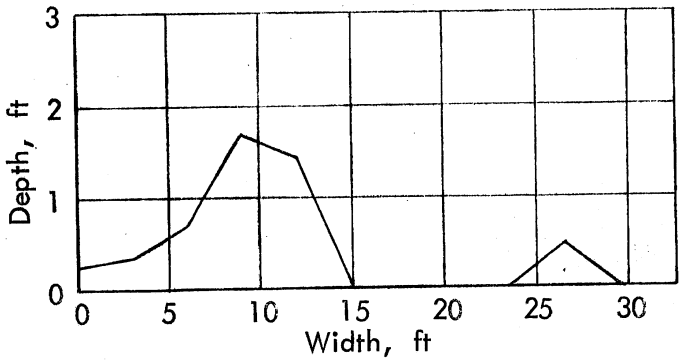

STATION 5

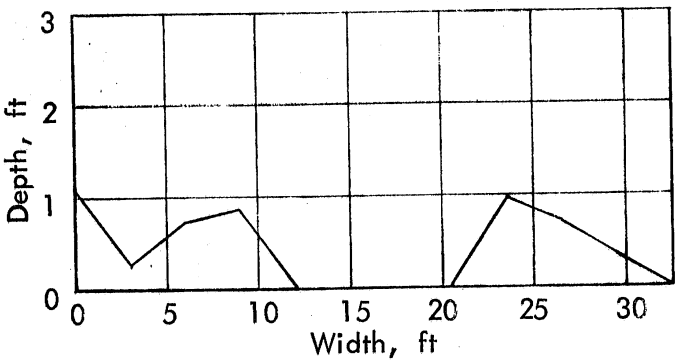

STATION 6

Fig. II-3 - Bed Profiles of Grit Deposit - Exp. 4
620 mgd, 2 mm grit, with sills

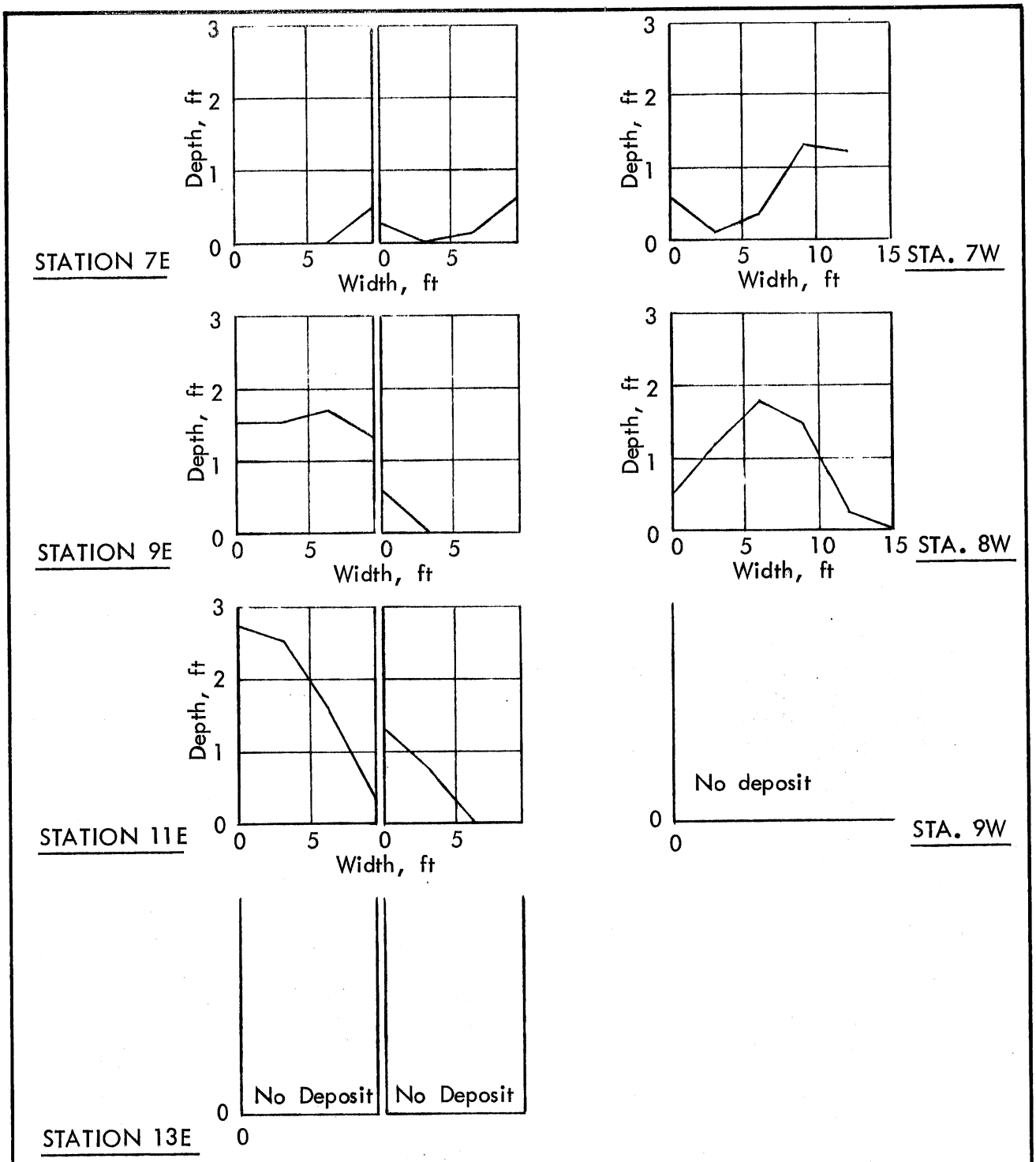

Fig. II-3 (Cont.) - Bed Profiles of Grit Deposit - Exp. 4
620 mgd, 2 mm grit, with sills

2. Flow and Grit Transport through Modified Structure

Series III: Alternative Modifications

To improve the hydraulic flow conditions in the diversion structure it was deemed necessary to prevent the formation of an undular hydraulic jump. This could be achieved by placing sills or baffle piers on the bottom of the diversion structure. Two types of sills placed either normal or at some angle to the flow were used tentatively. Better flow conditions could be achieved by using baffle blocks. Cylindrical baffle blocks were chosen because they are probably least susceptible to abrasion by suspended solids and clogging with large objects. Grit can pass between the blocks.

Two sizes of blocks were used, one 2.5 ft in diameter and 2.5 ft high and the other 4.4 ft in diameter and 3.0 ft high. Six of the smaller blocks performed about as well as four of the larger ones. The smaller blocks were chosen. The smoothest water surface was found when the centers of the cylindrical blocks were placed 49.25 ft downstream from the beginning of the diversion structure. The exact position and spacing chosen for the baffle blocks are shown in Fig. III-1.

Water surface profiles measured after installation of the blocks at a total flow of 620 mgd are shown in Figs. III-2 and III-3. Water depths in the old and new interceptors differ by no more than 0.6 ft. The improvement produced by the addition of the baffle blocks is considerable, as a comparison of Fig. III-2 with Fig. I-1 indicates. Turbulence and secondary currents induced by the baffle blocks were observed to produce a redistribution of water and grit. The cross flows in front of the wider pier were essentially eliminated and those in front of the narrower pier considerably weakened. No significant separation of the flow around the piers was observed. Grit was moved into both branches of the main interceptor. Patterns of grit deposition are shown in Figs. III-4 and III-5 for grit types 1 and 2 respectively. The patterns reflect the improved approach flow toward the piers. Experiments conducted under Series III showed a considerable improvement in flow conditions compared to Series I, but did not resolve the problem of grit deposition in both the old and the new branch of the main interceptor downstream of the branching point. Bed profiles recorded after approximately two hours of experimentation are shown in Figs. III-6 and III-7. A large wedge (dune) of grit material has been deposited at the beginning of the

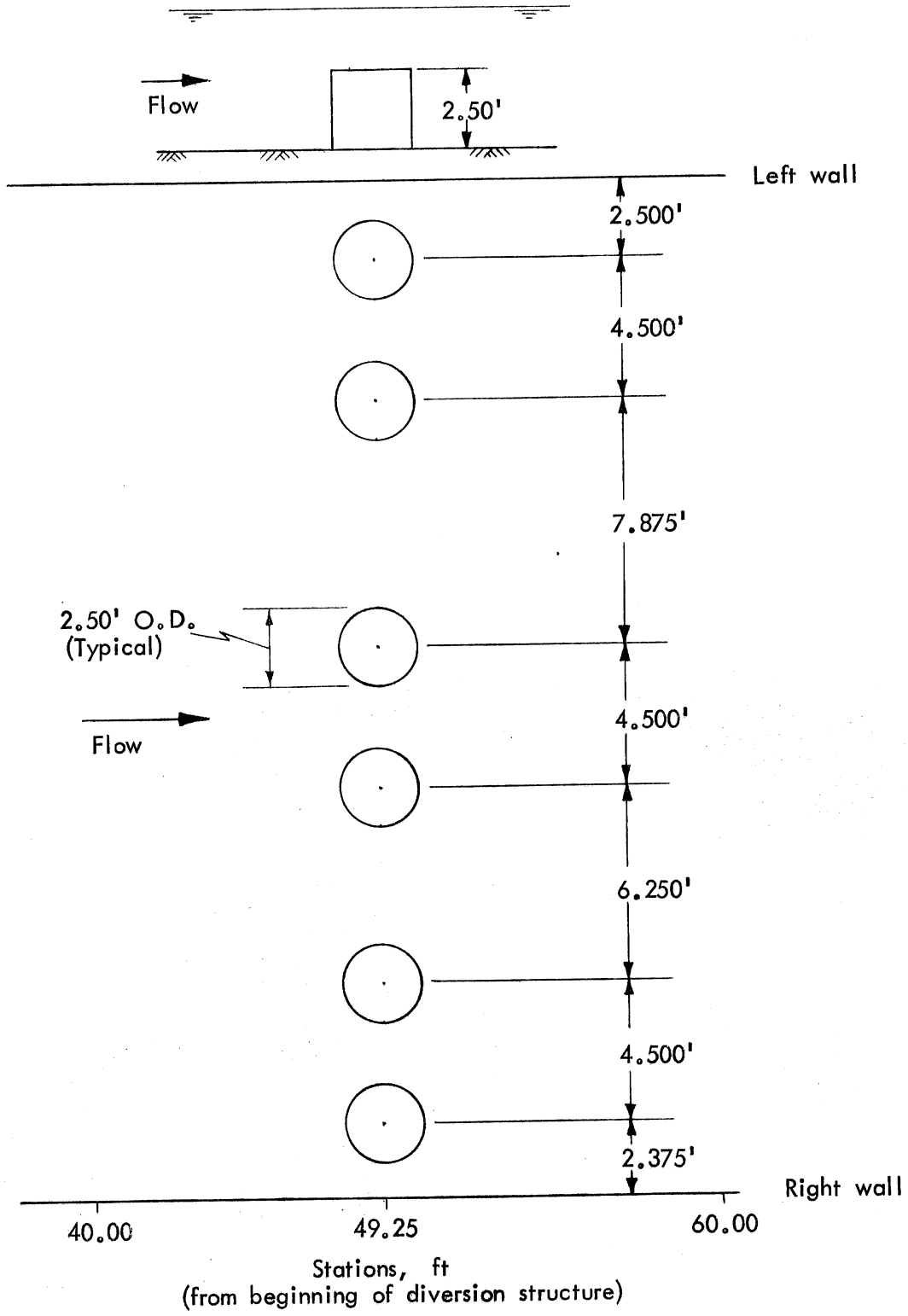

Fig. III-1 - Location of Baffle Blocks

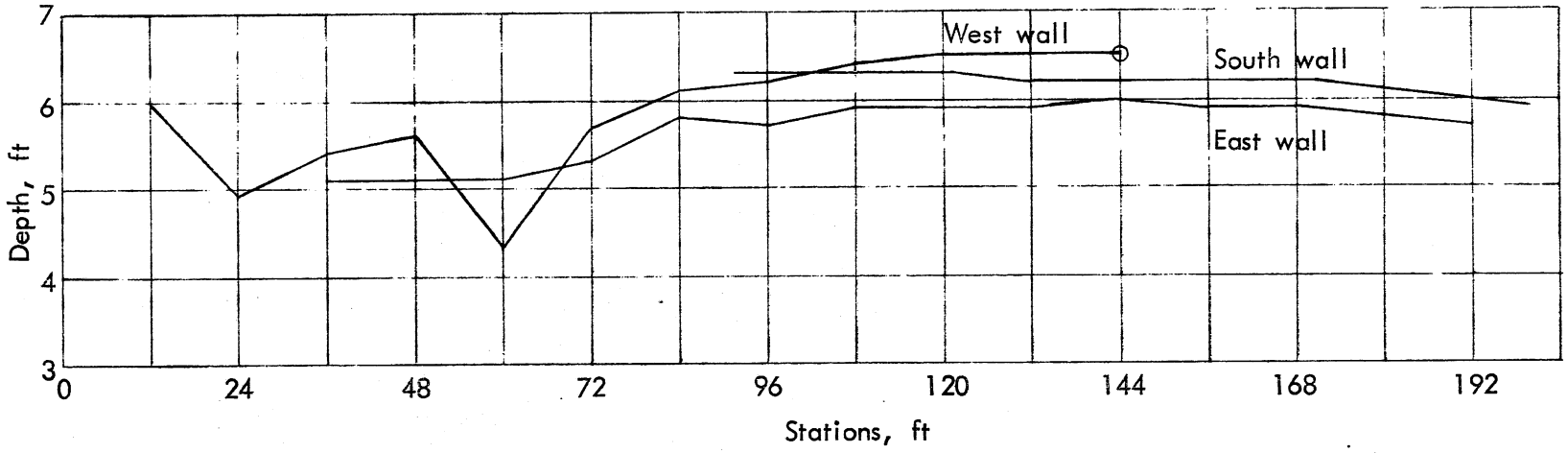

Fig. III-2 - Water Surface Profiles along Walls of Diversion Structure - Exp. 5
620 mgd, no grit, with baffle blocks

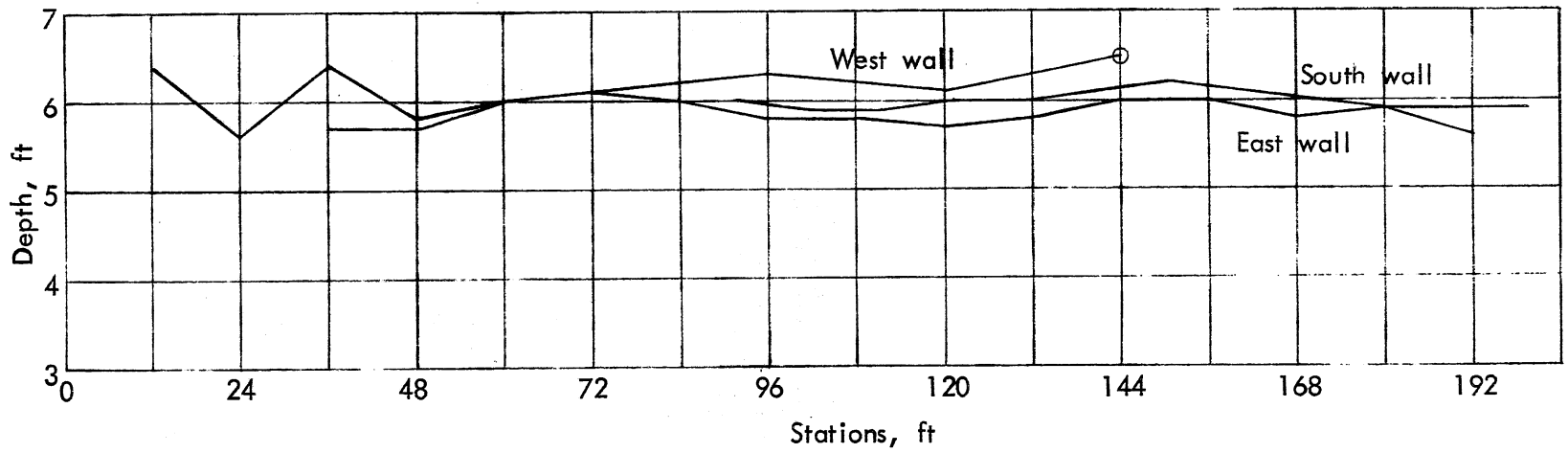

Fig. III-3 - Water Surface Profiles along Walls of Diversion Structure - Exp. 5
620 mgd, 2 mm grit, with baffle blocks

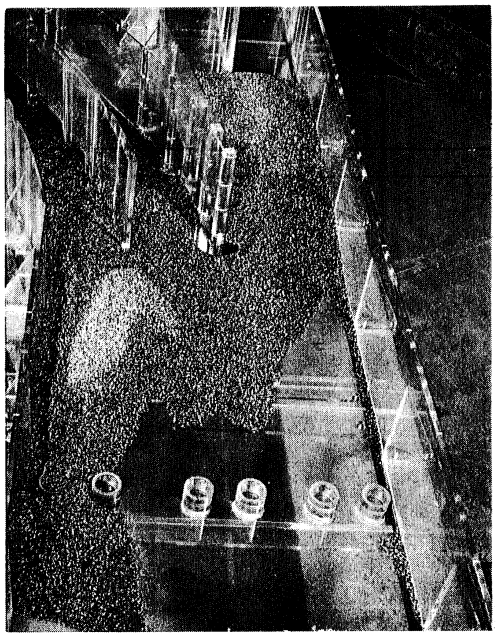

Fig. III-4 - Bed Deposits formed at 620 mgd with Grit Type 1 after Installation of Baffle Blocks (Series III)

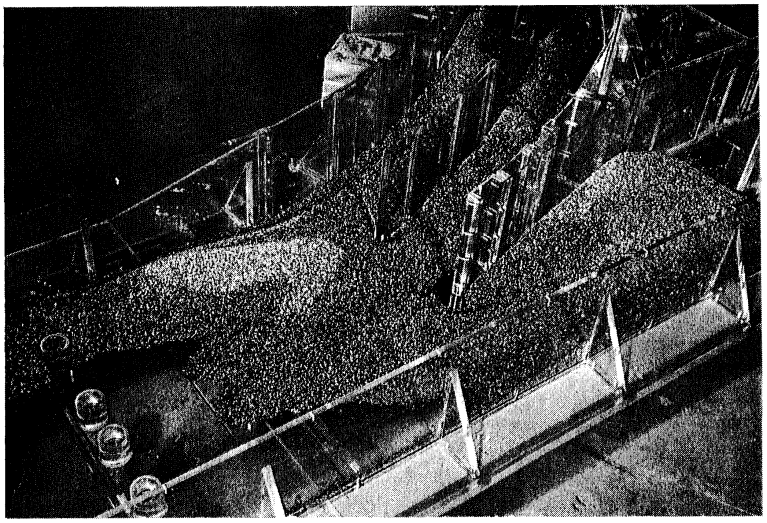

Fig. III-5 - Oblique View of Bed Deposits shown in Fig. III-4

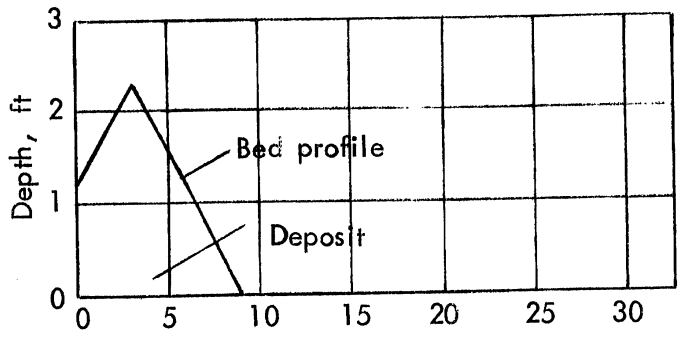

STATION 4

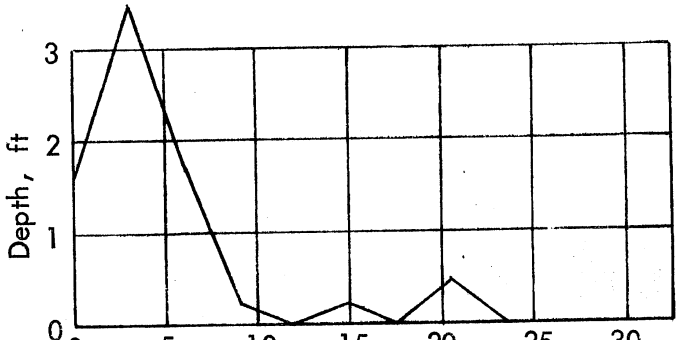

STATION 5

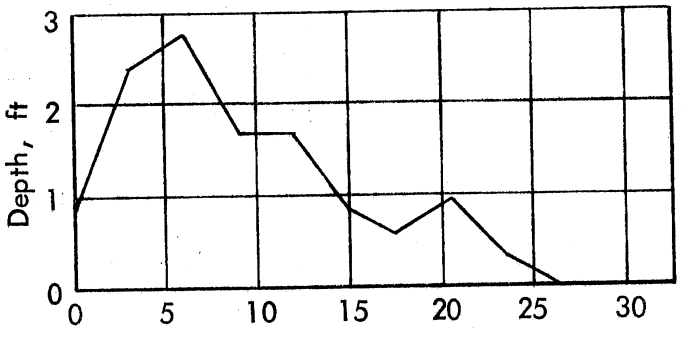

STATION 6

Fig. III-6 - Bed Profiles of Grit Deposit - Exp. 5
620 mgd, 2 mm grit, with baffle blocks

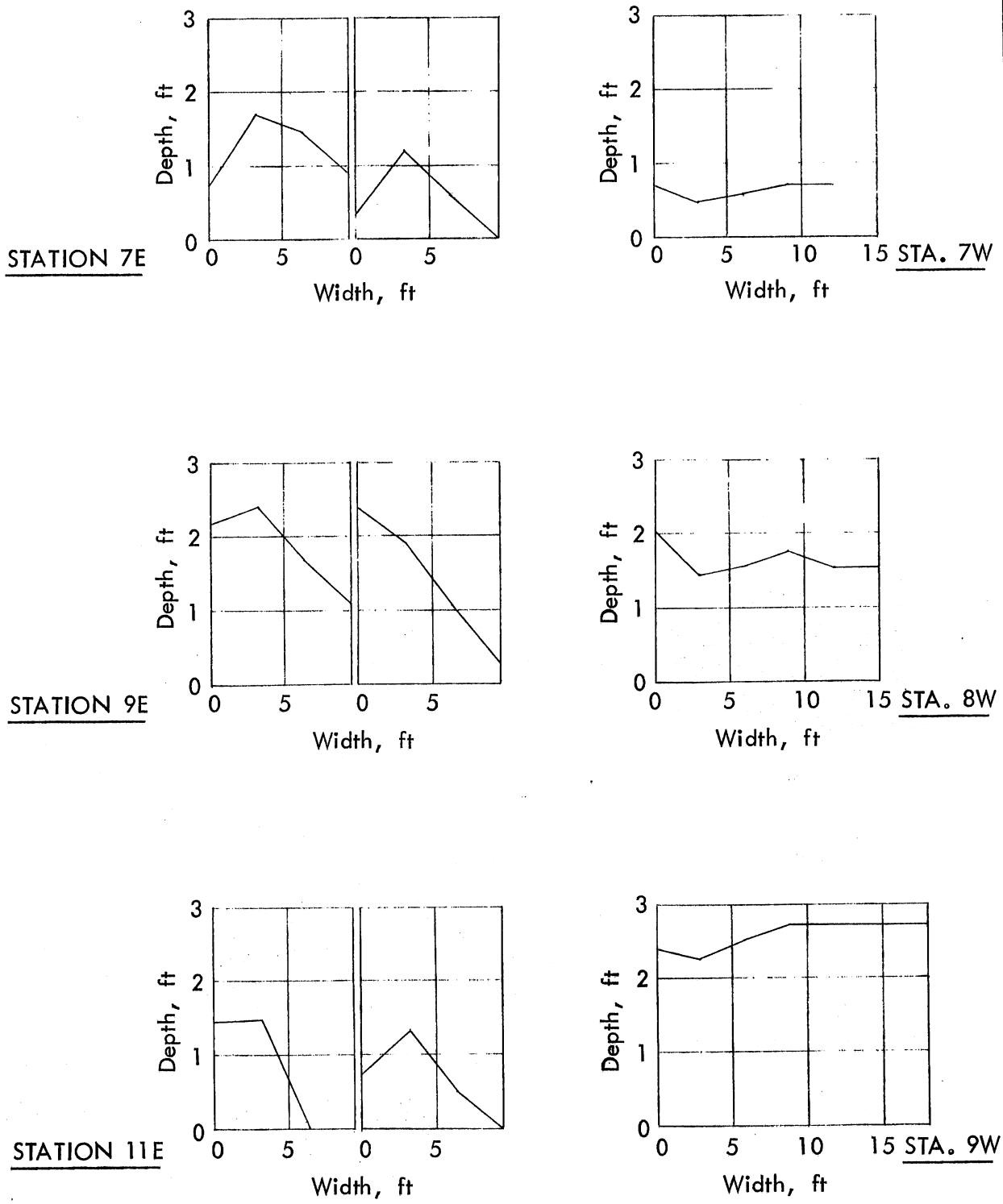

Fig. III-6 (Cont.) - Bed Profiles of Grit Deposit - Exp. 5
620 mgd, 2 mm grit, with baffle blocks

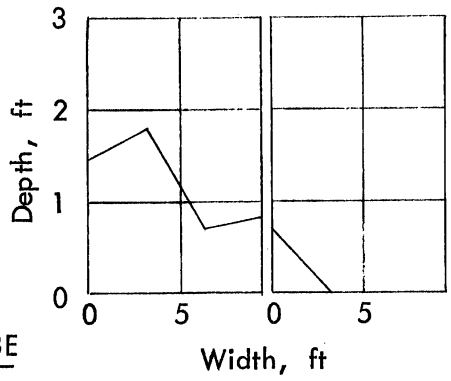

STATION 13E

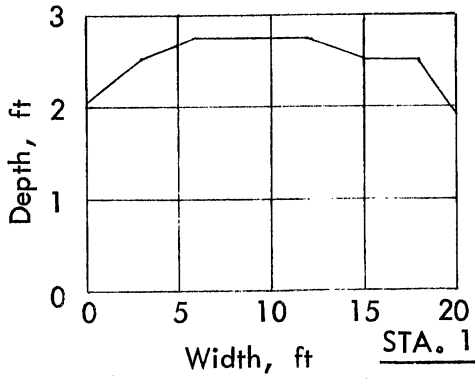

STA. 10W

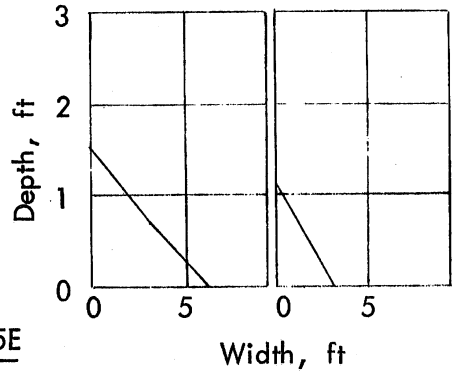

STATION 15E

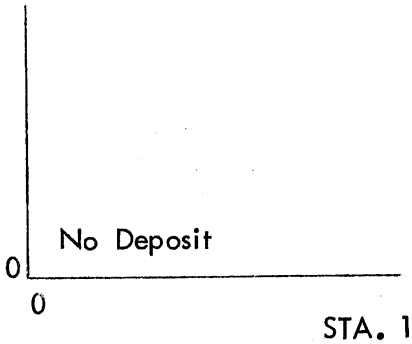

STA. 11W

Fig. III-6 (Cont.) - Bed Profiles of Grit Deposit - Exp. 5
620 mgd, 2 mm grit, with baffle blocks

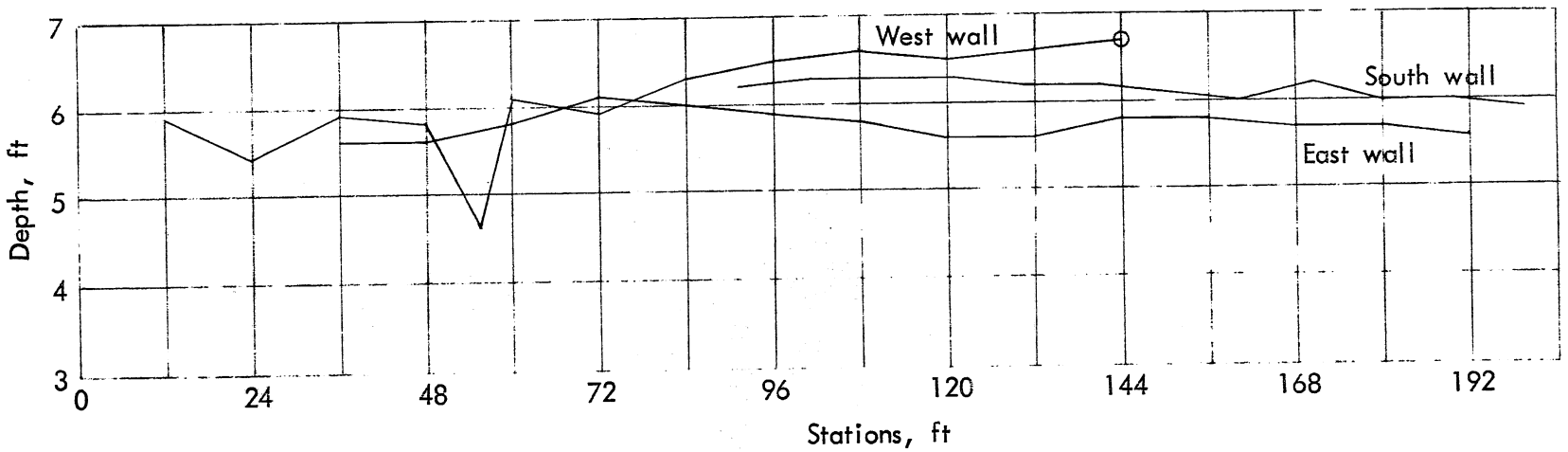

Fig. III-7 - Water Surface Profiles along Walls of Diversion Structure - Exp. 6
620 mgd, 0.7 mm grit, with baffle blocks

old interceptor and is moving downstream very slowly. The toe of the wedge is very near the front of the dividing pier. The wedge tends to deflect more of the grit toward the new interceptor. Consequently, 97 volume per cent of the total grit flux was recorded in the new branch interceptor while the deposition patterns were forming. True steady-state conditions for deposition patterns could not really be achieved. A considerable amount of grit was also deposited on the inside of the new branch interceptor; in the outside channel grit was readily moved along by the flow.

The results described in the preceding section were essentially duplicated in experiments using a fine grit size (type 2 instead of type 1). The results are shown in Fig. III-7 (water surface profiles), Figs. III-8 and III-9 (deposition patterns), and Fig. III-10 (bed profiles).

To examine the effect of deposition patterns on the distribution of grit fluxes, Experiment 7 was conducted with grit type 4 of low specific gravity. The same volume of grit was added at about the same volumetric rate as in the preceding experiment. It was found that 89 volume per cent of the grit went toward the new treatment plant and 11 volume per cent went toward the old plant. No significant amount of deposit occurred in Experiment 7.

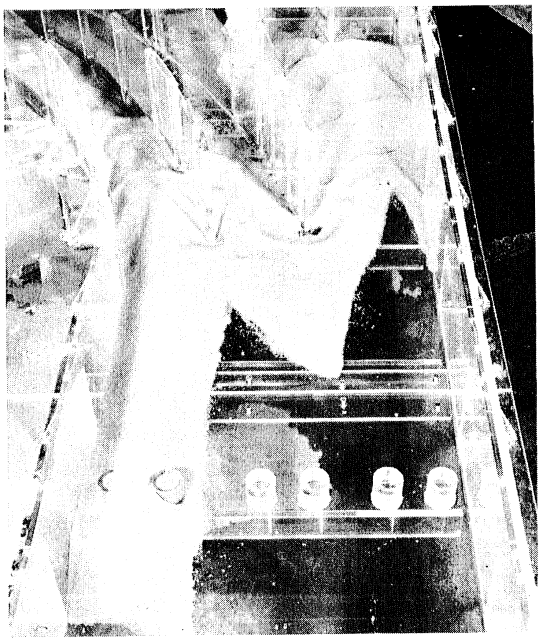

Fig. III-8 - Bed Deposits formed at 620 mgd with Grit Type 2 after Installation of Baffle Blocks (Series III)

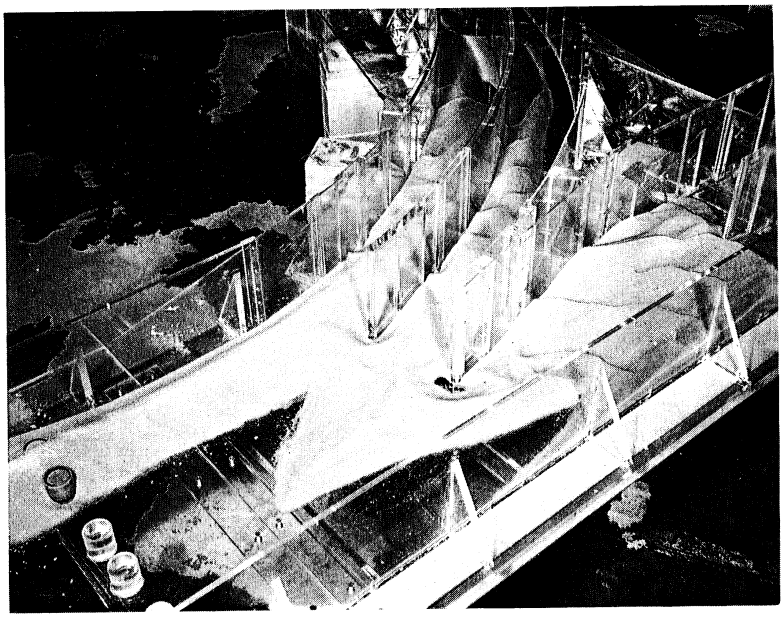

Fig. III-9 - Oblique View of Bed Deposits shown in Fig. III-8

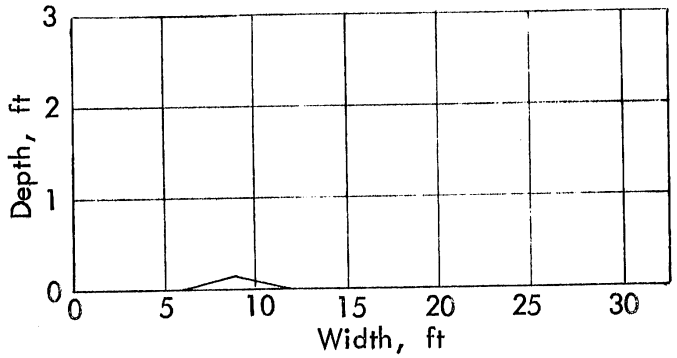

STATION 3

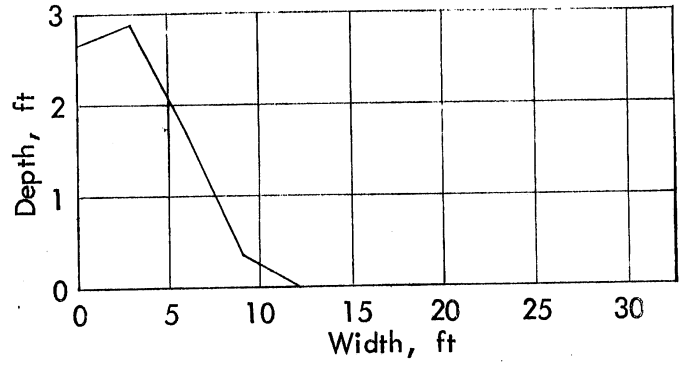

STATION 4

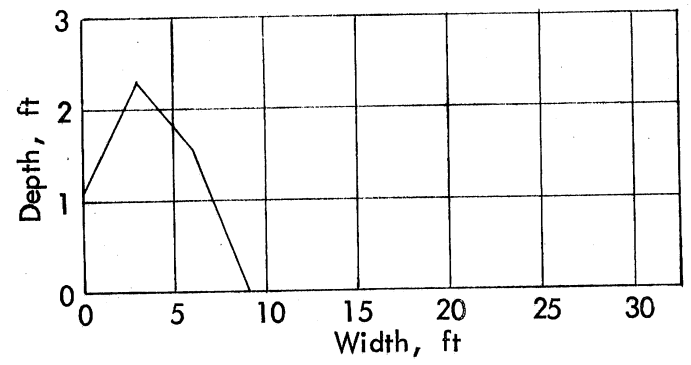

STATION 5

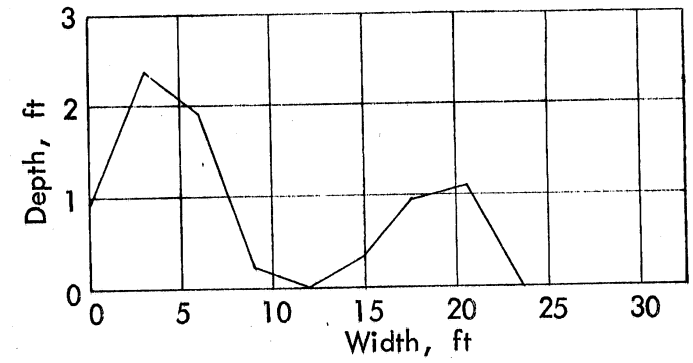

STATION 6

Fig. III-10 - Bed Profiles of Grit Deposit - Exp. 6
620 mgd, 0.7 mm grit, with baffle blocks

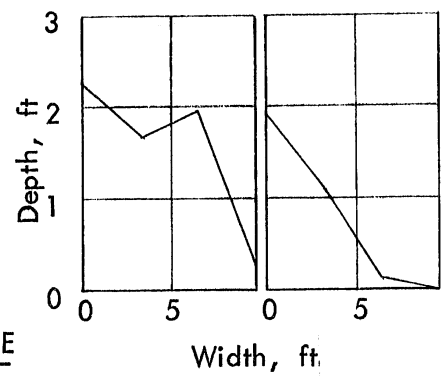

STATION 13E

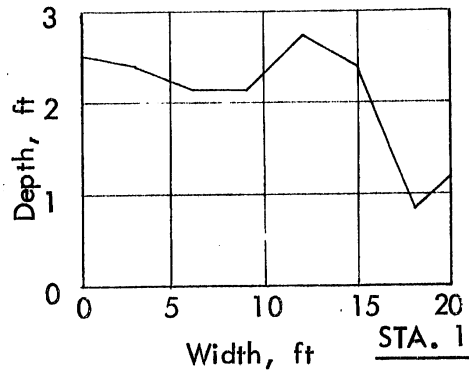

STA. 10W

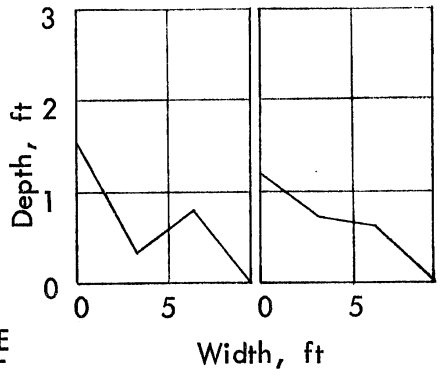

STATION 15E

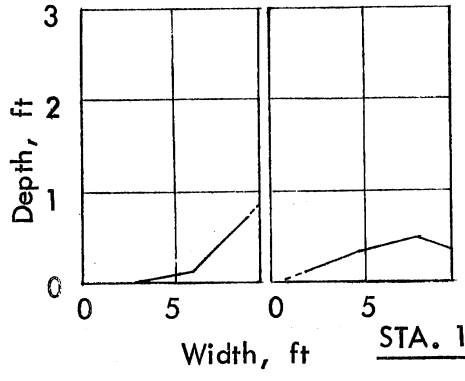

STA. 11W

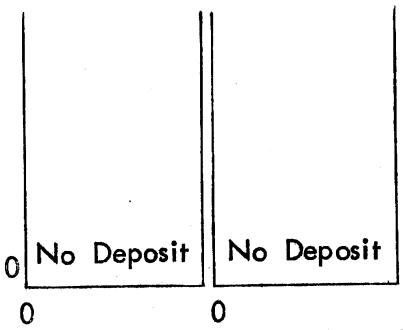

STA. 12W

Fig. III-10 (Cont.) - Bed Profiles of Grit Deposit - Exp. 6
620 mgd, 0.7 mm grit, with baffle blocks

Series IV: Proposed Modified Design

Series IV was conducted to determine whether the selected design was suitable for flow rates of less than the maximum flow (620 mgd). Four additional experiments were conducted with flow rates of 490, 273, and 176 mgd. Grit types 1 and 4 were used selectively. Water surface profiles were found to be acceptable in all cases. Grit distribution between the old and the new interceptor branch was found to be in the desirable range for the two larger flows (no measurements could be obtained for the 176 mgd flow). Details of measured water surface profiles are shown in Figs. IV-1 through IV-3. Water depths throughout the diversion structure become more uniform as the total flow is decreased.

Deposition patterns obtained for the 176 mgd flow are shown in Figs. IV-4 and IV-5. Grit type 4 was used. Bed profiles are given in Fig. IV-6. The patterns and profiles bear similarity to those obtained with the 620 mgd flow and grit type 1. In particular, it is again observed that the grit settles preferentially at the beginning of the old interceptor branch (diverging channel section).

No deposition patterns could be obtained for the intermediate flows of 490 and 273 mgd, because grit type 4 would not settle and grit types 1 through 3 would not be transported at significant rates. It was observed, however, that grit type 4 followed very similar paths for all flow conditions.

The distribution of grit between the old (existing) and the projected interceptor branches, as measured in volume percentages using the amount of material collected in the sediment trap at the end of each channel, is summarized in Table IV-1. By comparison, dissolved or very fine suspended material will be divided in the same proportion as the total flow. The distribution is 58 per cent toward the new plant and 42 per cent toward the existing plant. Table IV-1 therefore consistently shows that with increasing resistance to transport, grit has a tendency to be moved toward the new treatment facilities. The possible range of relative grit volume to be found in the new branch interceptor is from 58 to 100 per cent if transport both in suspension and as bed load is considered. The experimental data in Table D-1, Appendix D suggest strongly that grit transported as bed load will be diverted into the new branch interceptor at a rate most likely exceeding 75 per cent of the total bed load.

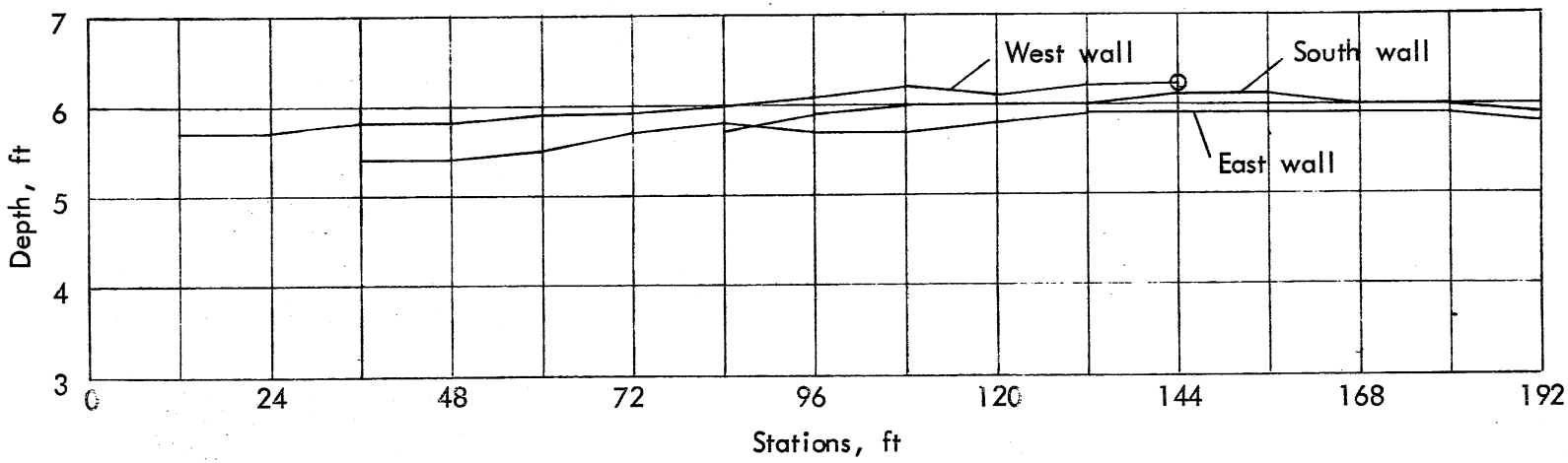

Fig. IV-1 - Water Surface Profiles along Walls of Diversion Structure - Exp. 9
490 mgd, no grit, with baffle blocks

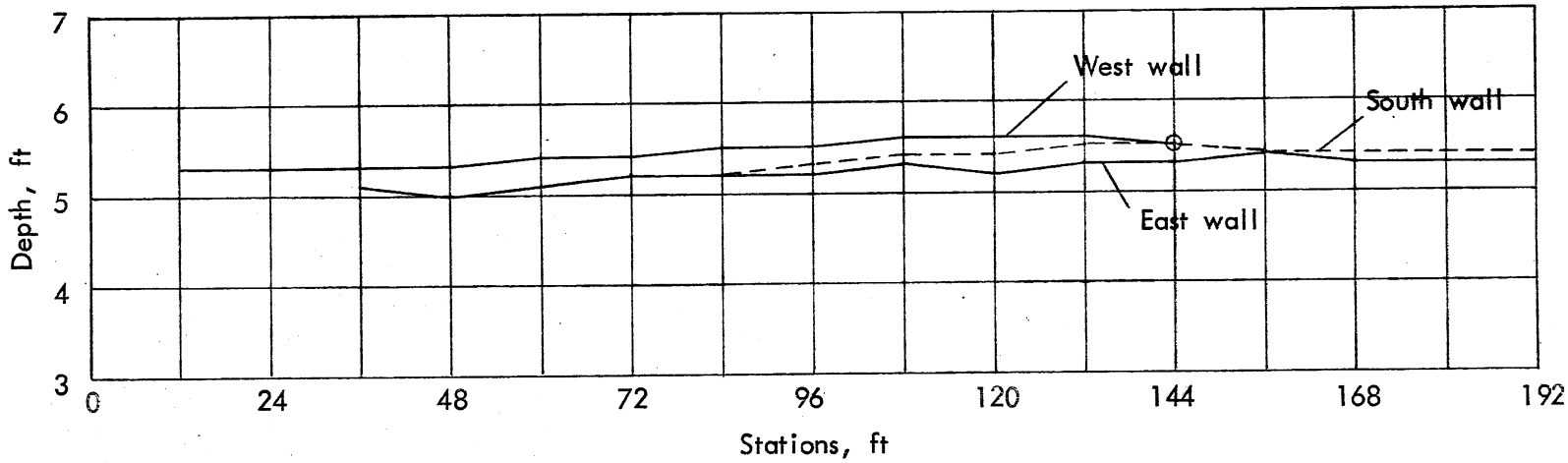

Fig. IV-2 - Water Surface Profiles along Walls of Diversion Structure - Exp. 10
273 mgd, no grit, with baffle blocks

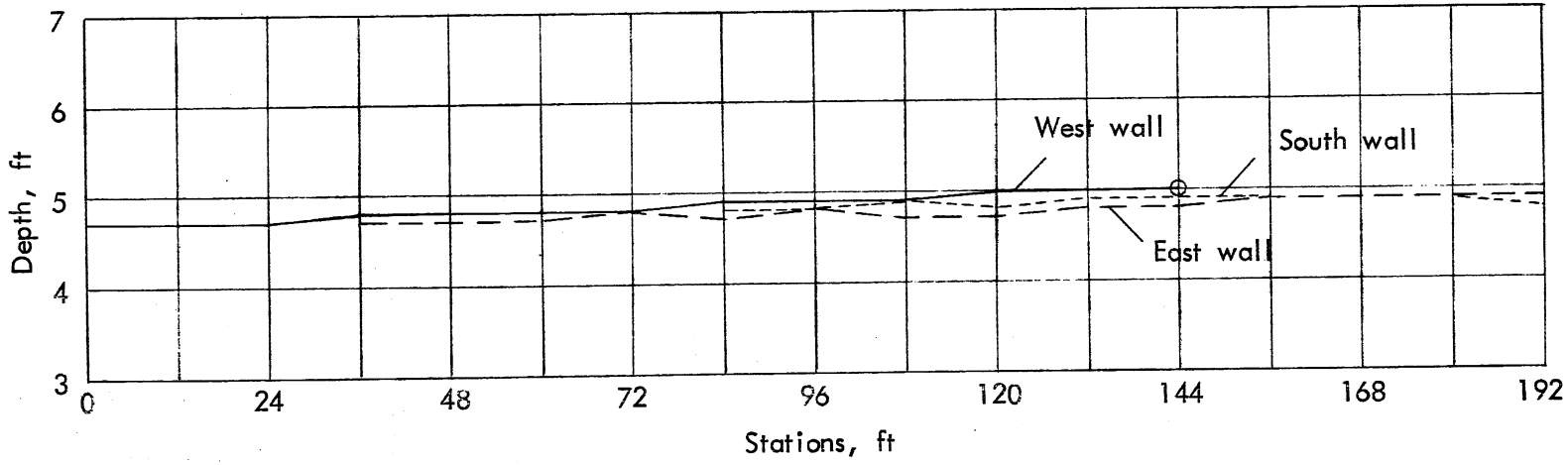

Fig. IV-3 - Water Surface Profiles along Walls of Diversion Structure - Exp. 11
176 mgd, no grit, with baffle blocks

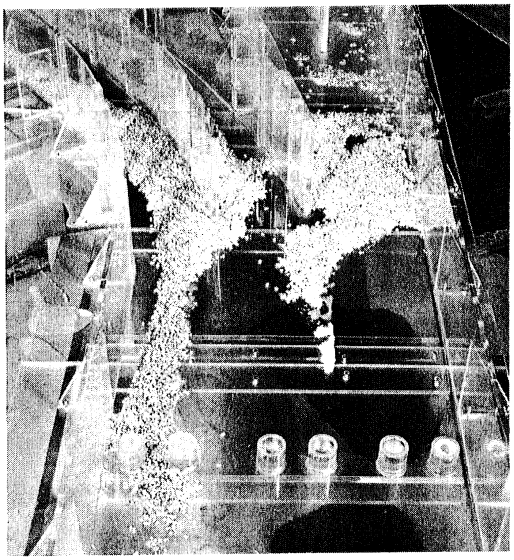

Fig. IV-4 - Bed Deposits formed at 176 mgd with Grit Type 4 (Series IV)

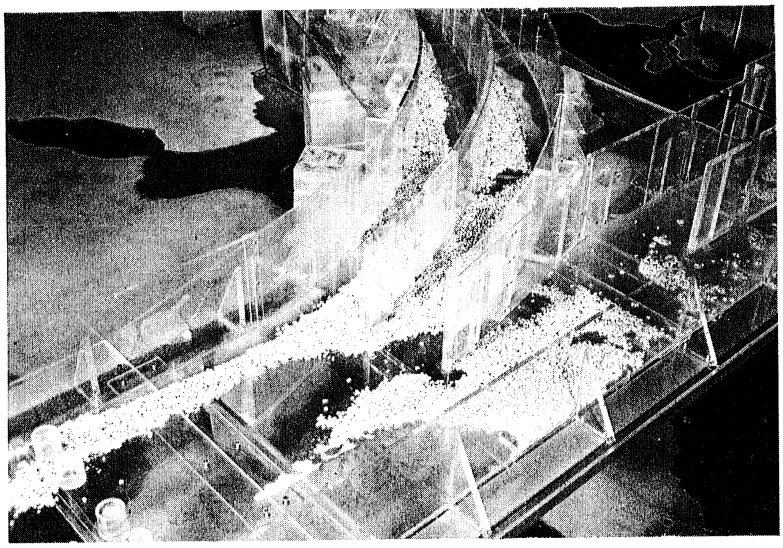

Fig. IV-5 - Oblique View of Bed Deposits shown in Fig. IV-4

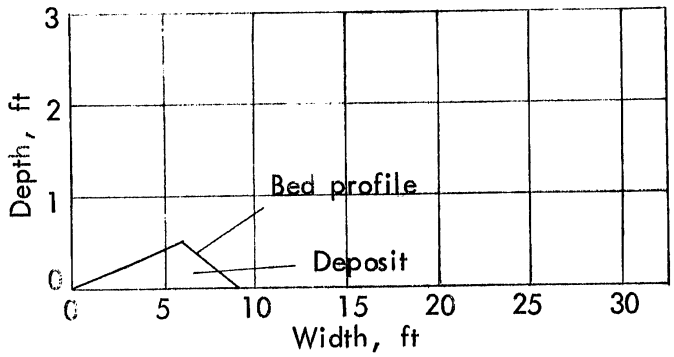

STATION 4

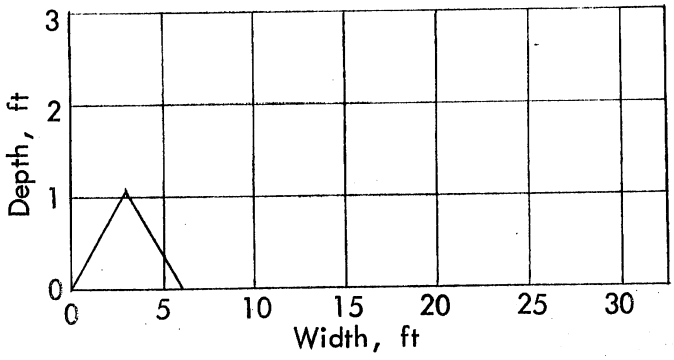

STATION 5

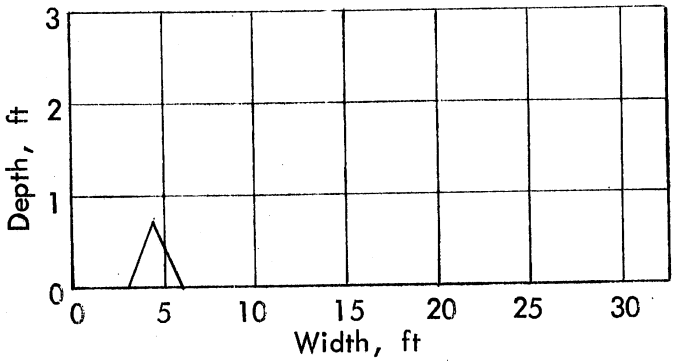

STATION 6

Fig. IV-6 - Bed Profiles of Grit Deposit - Exp. 11
176 mgd, type 4 grit (corn), with blocks

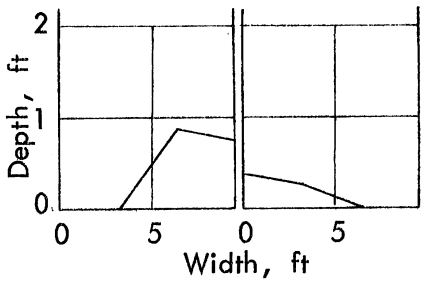

STATION 7E

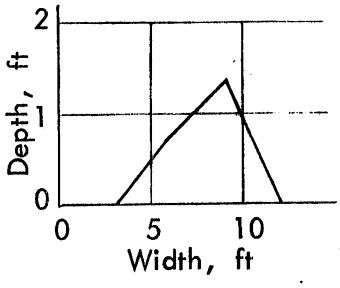

STA. 7W

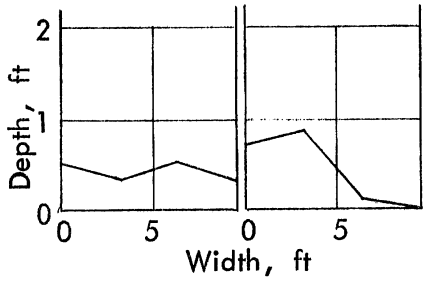

STATION 9E

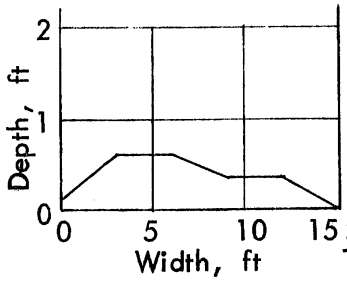

STA. 8W

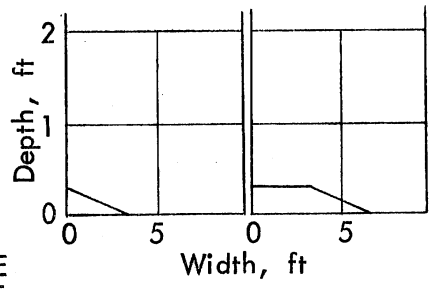

STATION 11E

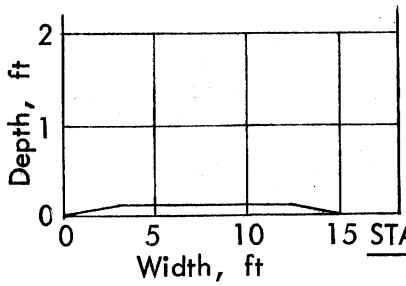

STA. 9W

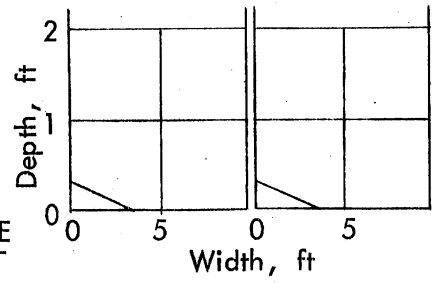

STATION 13E

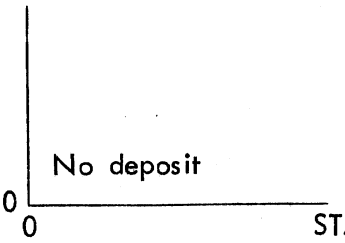

STA. 10W

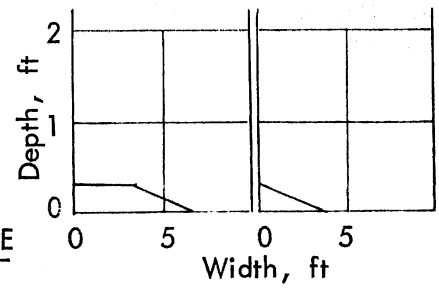

STATION 15E

Fig. IV-6 (Cont.) - Bed Profiles of Grit Deposit - Exp. 11
176 mgd
Type 4 grit (corn)
With blocks

Series V: Operation with Three Approach Barrels

The overall layout of the diversion structure, as seen in Fig. 1, incorporates a future addition of a third main interceptor barrel to the east of the existing two. It therefore seemed reasonable to examine in the model the hydraulic flow conditions and the grit distribution to be expected after addition of the third barrel. An experiment was conducted for a total flow of 930 mgd, of which 668 mgd were routed toward the new treatment facility and 262 toward the existing plant (flow condition E in Table A-1). Grit type 4 was used.

Measured water surface profiles as reported in Fig. V-1 indicate the imposed water depth of 7.7 ft in the existing interceptor barrel and depths of only 5.8 and 6.0 ft at the end of the 90° bend of the new branch interceptor. The very substantial difference in depth of nearly 2 ft is caused by the much larger proportion of the total flow in the new branch interceptor. It was found that 88 per cent of the type 4 grit moved into the new branch interceptor and only 12 per cent moved into the existing one. As expected, no deposition was observed with grit type 4.

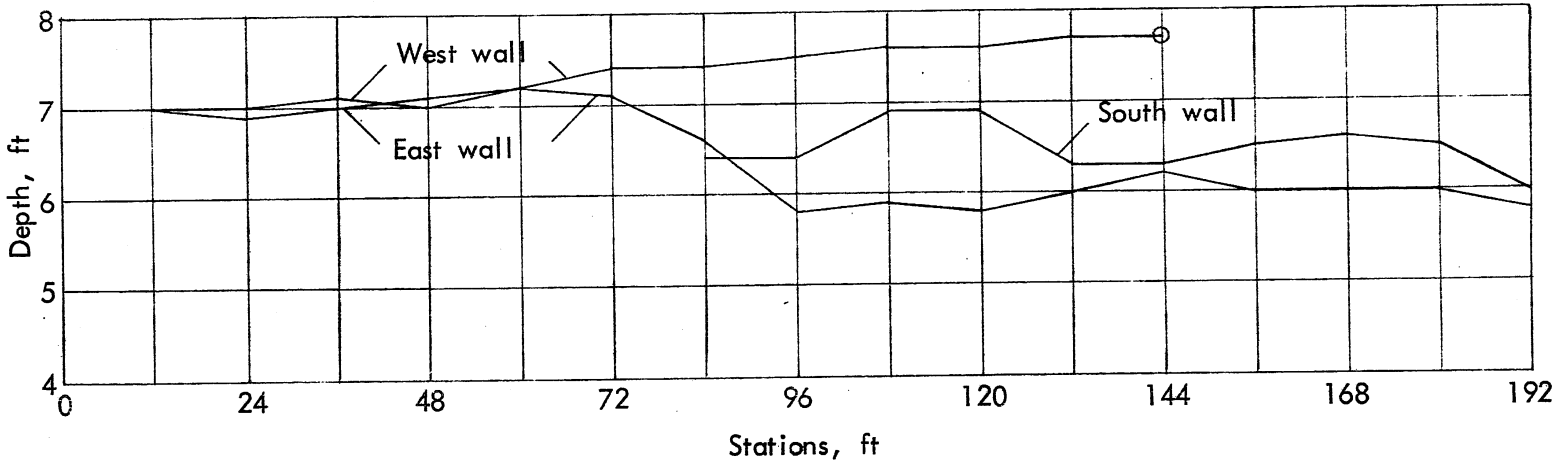

Fig. V-1 - Water Surface Profiles along Walls of Diversion Structure - Exp. 12
930 mgd, no grit, with baffle blocks

Series VI: Operation with Two of Four Downstream Barrels Closed

The deposition of grit in the interceptor downstream of (and in) the diversion structure is a very natural phenomenon and can hardly be prevented without reducing the flow cross sections. Average flow velocities in the four barrels of the branch interceptors are substantially less than in the two barrels of the original main interceptor. The loss in tractive force (bed shear stress) associated with a reduction in flow velocity causes deposition of bed material. This will most likely also occur in the prototype. Grit deposits accumulating in the interceptor barrels downstream of the diversion structure may have a detrimental effect on flow and plant operation, for example through increases in headloss and water surface elevation. It was therefore believed necessary to investigate whether closing two of the four downstream barrels, using the gates already provided for, could prevent or reduce total sediment deposit in the diversion structure and the downstream barrels.

Experiments were conducted with either the left or the right barrel in each branch fully gated. Grit types 1 and 4 were applied with a flow of 620 mgd, which had produced the most adverse flow conditions in all previous experiments.

Closing of the barrels has a very significant effect on water depths. A downstream depth of 7.1 ft was imposed in the existing interceptor. That value was provided by the project sponsor as a result of backwater curve computations. Measured water surface profiles are shown in Figs. VI-1 and VI-2. Water depths within the diversion structure reach 8 ft, but at the end of the structure water depths in the open barrels are 6.9 ft and 7.1 ft if the left barrel in each branch is closed and 6.7 and 7.1 ft if the right barrels are closed.

It is very important to note that it was not found possible to divide the 620 mgd flow in the desired proportions of 58 and 42 per cent of the total flow. With the left barrel in each branch closed, 54 per cent (335 mgd) and 46 per cent (285 mgd) could be routed into the new and the old branch, respectively. With the right barrel in each branch closed the distribution of water was 51 per cent (316 mgd) and 49 per cent (304 mgd), respectively, into the new and the old branch. The reason for this is a critical flow condition at the beginning of the barrel leading toward the new treatment facilities. In other words, the flow in that barrel is inlet

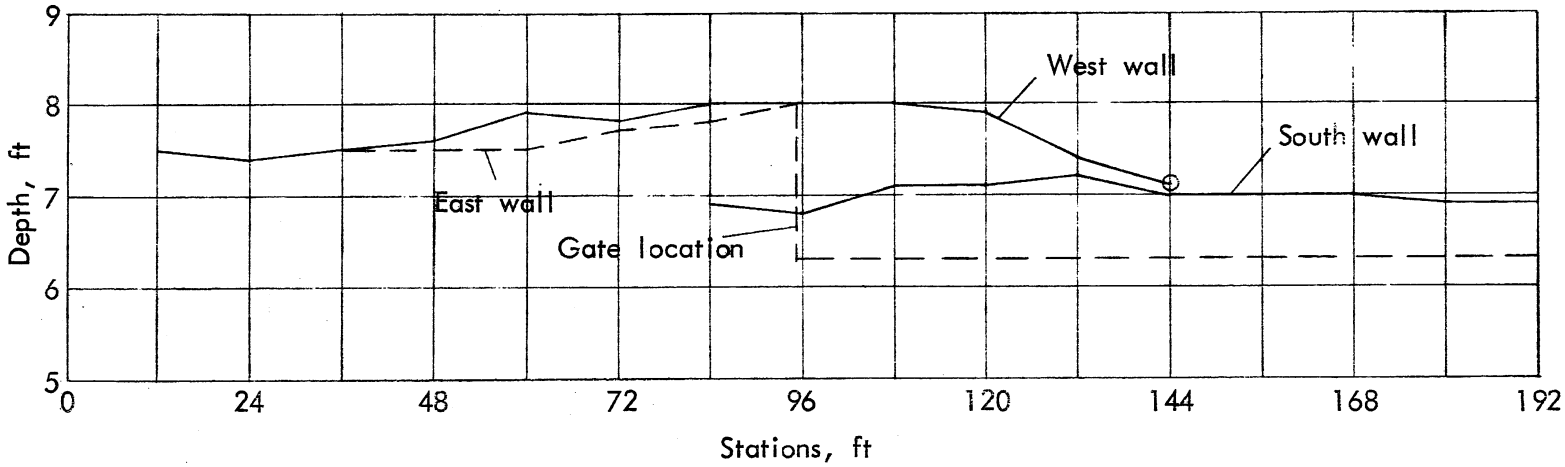

Fig. VI-1 - Water Surface Profiles along Walls of Diversion Structure - Exp. 14
620 mgd, no grit, with baffle blocks and left barrel in each
downstream branch fully gated

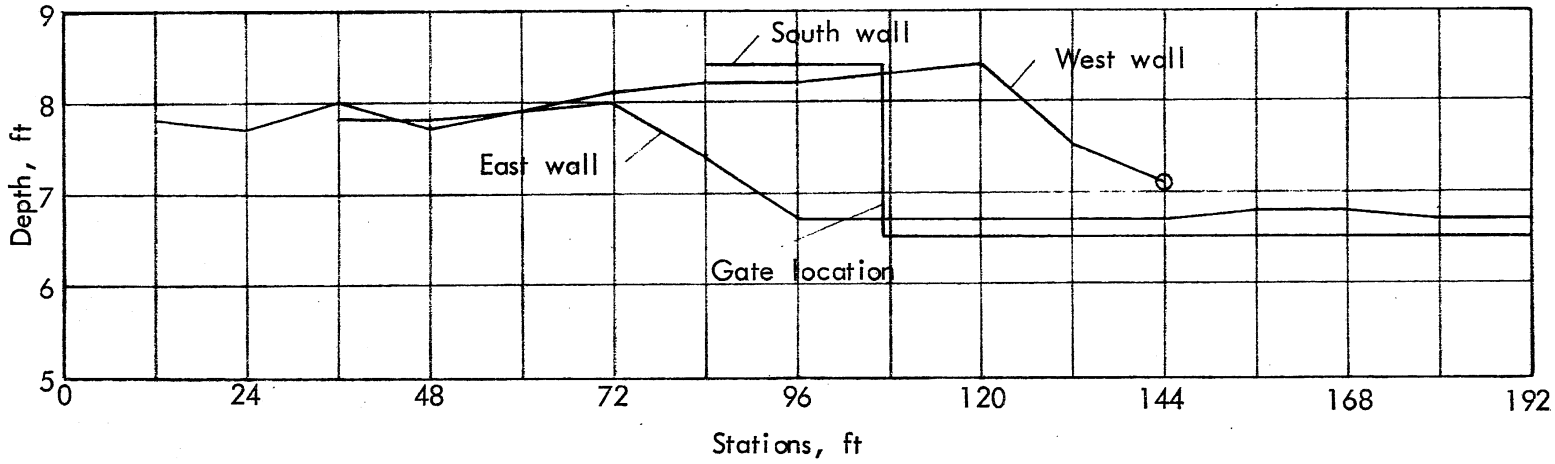

Fig. VI-2 - Water Surface Profiles along Walls of Diversion Structure - Exp. 15
620 mgd, no grit, with baffle blocks and right barrel in each downstream branch fully gated

controlled. Assuming a contraction coefficient of the order of 0.8, it can be shown that the inlet flow will indeed be a critical flow.

This situation could be improved by imposing a depth on the order of 7.7 ft instead of 7.1 ft through downstream control in the existing (old) branch.

Grit deposition in the barrels was effectively eliminated by closing two of the four. Within the confines of the diversion structure itself a substantial amount of deposit still occurred when grit type 1 was used. This can be seen in Figs. VI-3 and VI-4 for the left barrel closed in each branch and in Figs. VI-5 and VI-6 for the right barrels closed. When the pictures were taken (approximately 4 hours after the beginning of the experiment), grit was still being deposited in the areas shown, indicating that no equilibrium had been reached for the bed load transport. Measured bed profiles associated with Figs. VI-3 through VI-6 are given in Figs. VI-7 and VI-8.

This finding must be interpreted as an indication that within the diversion structure the heaviest grit particles may accumulate continuously simply because of the geometry of the structure and regardless of the mode of operation. Grit distributions were measured with grit type 4 with the results given in Table D-2 of Appendix D. These results reflect an adequate grit distribution.

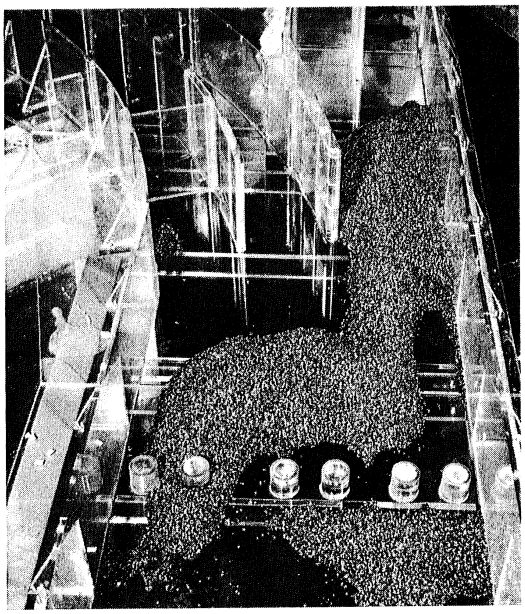

Fig. VI-3 - Bed Deposits formed at 620 mgd with Left Downstream Barrels Closed and Grit Type 1 (Series VI)

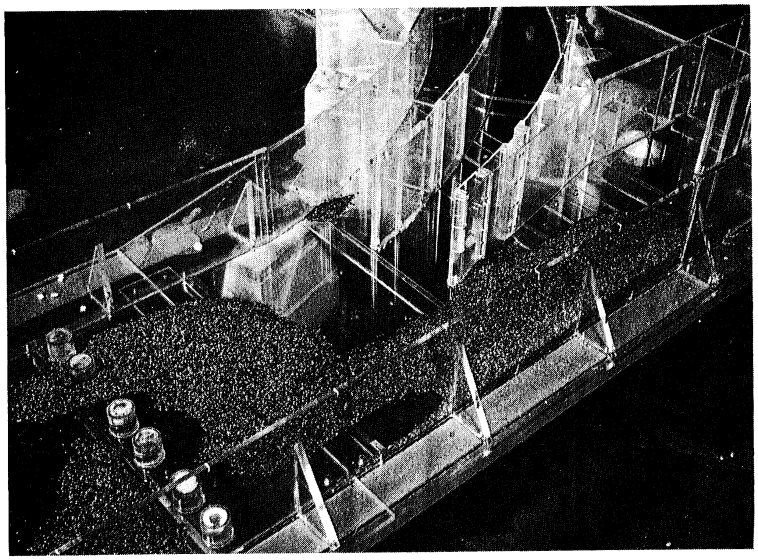

Fig. VI-4 - Oblique View of Bed Deposits shown in Fig. VI-3

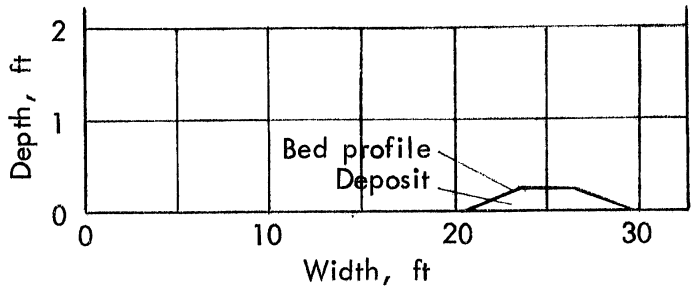

STATION 3

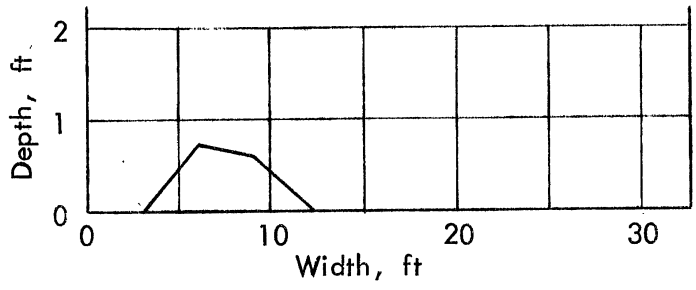

STATION 4

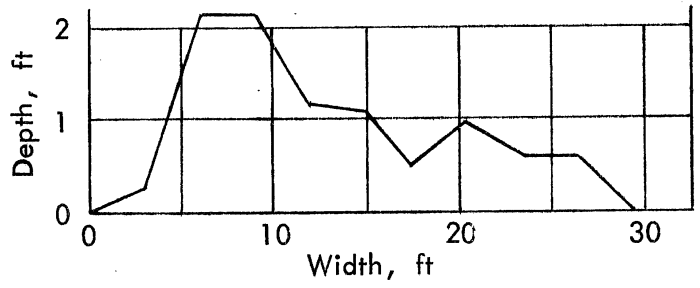

STATION 5

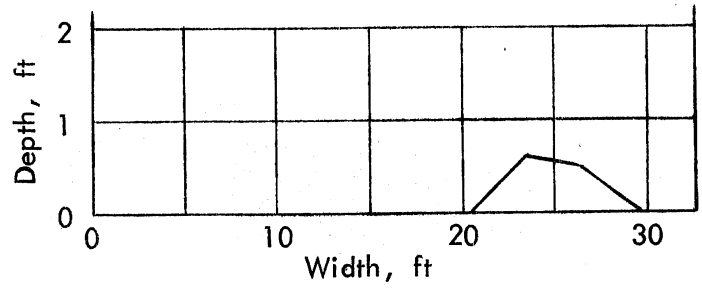

STATION 6

Fig. VI-7 - Bed Profiles of Grit Deposit - Exp. 16
620 mgd, 2 mm grit, with baffle blocks and left barrel in each branch fully gated

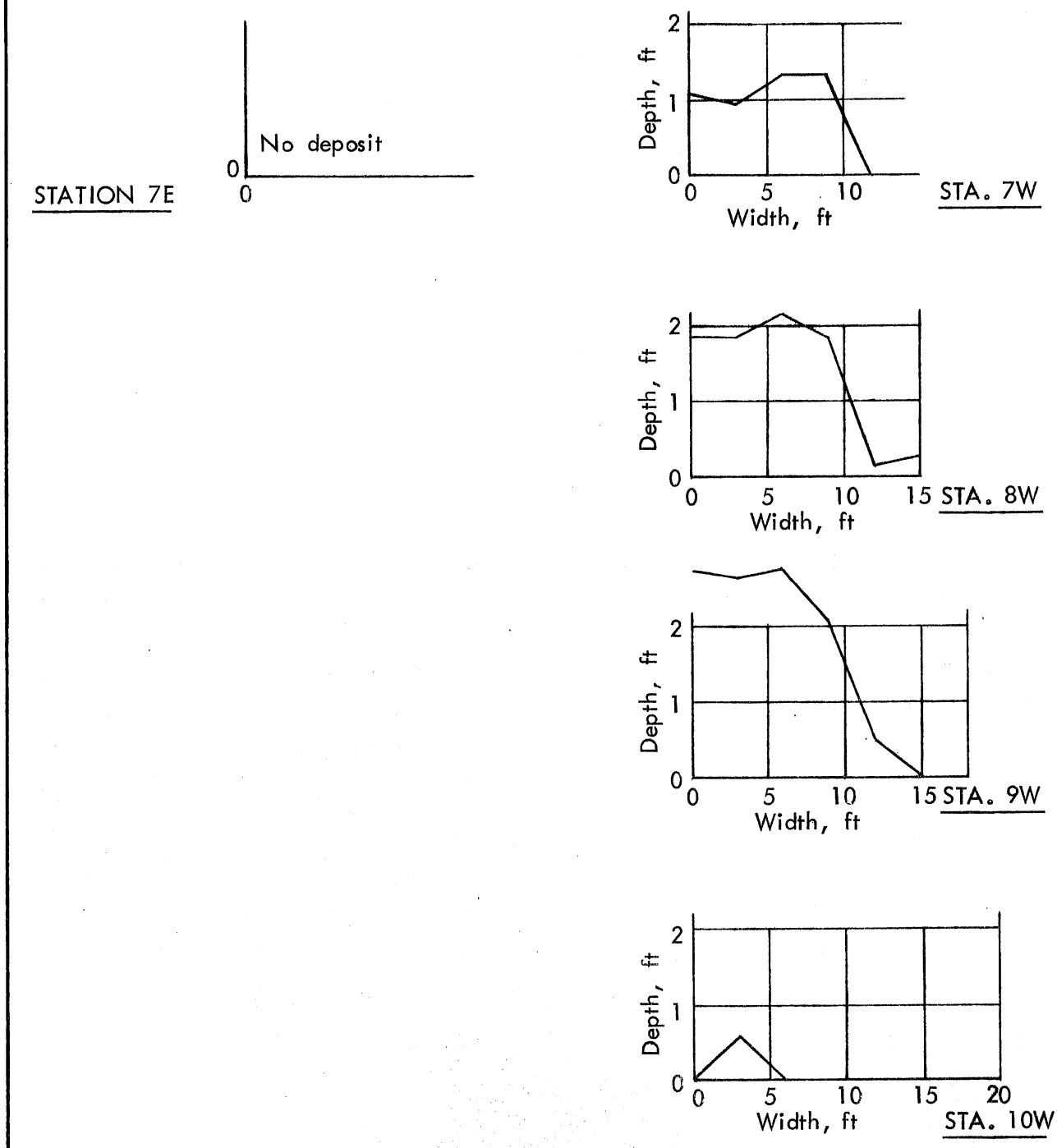

Fig. VI-7 (Cont.) - Bed Profiles of Grit Deposit - Exp. 16
620 mgd, 2 mm grit, with baffle blocks
and left barrel in each branch fully
gated

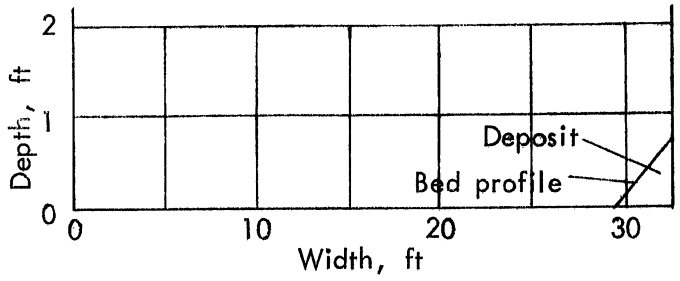

STATION 3

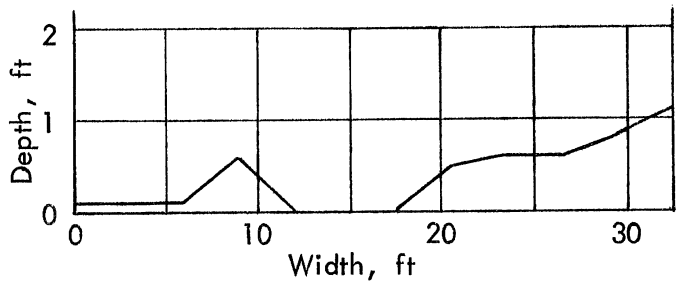

STATION 3.5

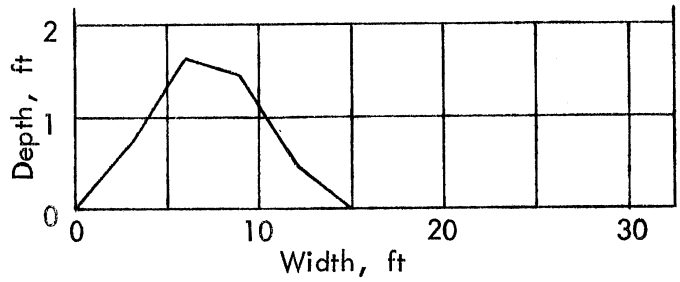

STATION 4

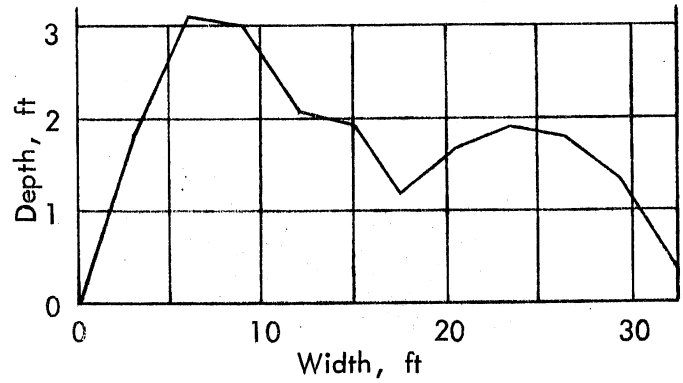

STATION 5

Fig. VI-8 - Bed Profiles of Grit Deposit - Exp. 17
620 mgd, 2 mm grit, with baffle blocks
and right barrel in each branch fully
gated

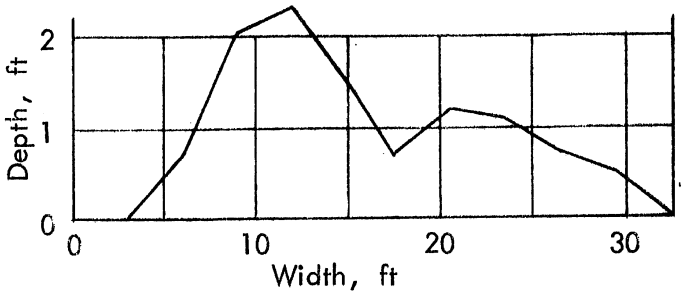

STATION 5.5

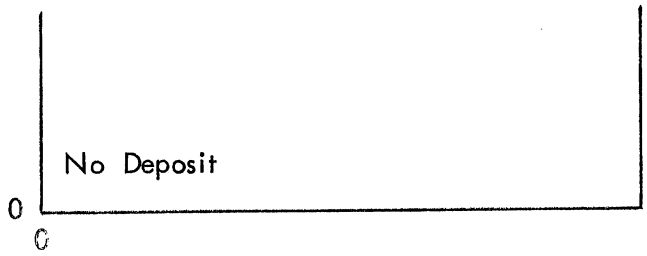

STATION 6

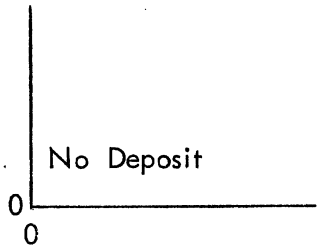

STATION 7E

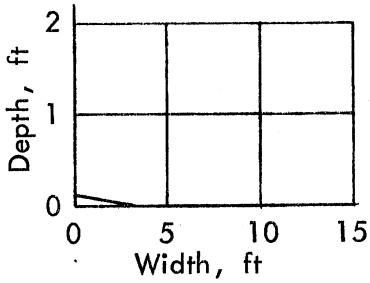

STA. 8W

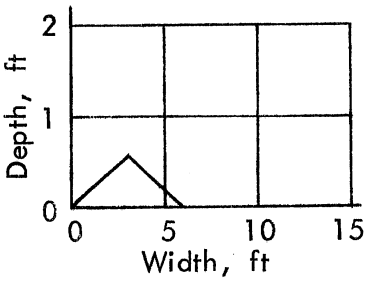

STA. 8.5W

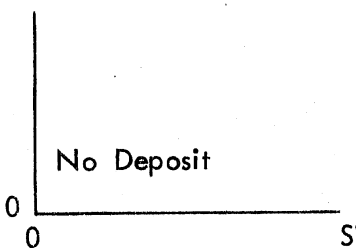

STA. 9W

Fig. VI-8 (Cont.) - Bed Profiles of Grit Deposit - Exp. 17
620 mgd, 2 mm grit, with baffle blocks
and right barrel in each branch fully
gated

3. Headlosses in Modified Structure

Flow in the main interceptor barrels downstream of the diversion structure will be subcritical with the exception of the conditions described under Series VI. Weirs or gates installed at the end of either interceptor branch will control the water level in the diversion structure and the distribution of the total flow. Backwater computations starting with known or assumed water elevations at the downstream weirs or gates and known flow rates in each branch must tie in with the water depths measured in the model study at the downstream end of the diversion structure. If, for any reason, backwater curves have to be evaluated through the diversion structure, the depth measurements reported in the preceding section can be used. As an alternative to the direct use of model water depths, a headloss coefficient for the diversion structure can be found from the model measurements. Actually, two separate coefficients must be used. They are defined by the relationships

$$h_E = \lambda_E \frac{V_1^2}{2g} \quad \text{and}$$

$$h_W = \lambda_W \frac{V_1^2}{2g}$$

where h_E is the headloss between stations 1 and 16E in the new (east) branch, h_W is the headloss between stations 1 and 12W in the old (west) branch (see Fig. 13 for station identification), λ_E and λ_W are the corresponding headloss coefficients, and V_1 is the average velocity of approach (at station 1) into the diversion structure.

The selection of $V_1^2/2g$ as reference velocity head has some physical significance, because a portion of the total headloss is caused by the sudden flow expansion at the beginning of the diversion structure and the baffle piers. These losses depend on V_1 and are properly modeled by Froude similarity. Headlosses by wall friction are modeled in the ratio of shear stresses. Using shear stress values from Tables A-2 and B-1, the model: prototype ratio of bed shear stresses ranges from 1:11.3 to 1:13.3, which is fairly close to the geometrical scale ratio of 1:12. It can therefore be expected that the model will provide representative values of headlosses even though Reynolds similarity is not strictly satisfied.

Headlosses h_E and h_W were derived from measurements of flow depths and flow rates in each branch. The relationships actually used are

$$h_E = H_1 - H_{16E} = \alpha\left(\frac{V_1^2}{2g} - \frac{V_{16E}^2}{2g}\right) + (y_1 - y_{16E}) + (z_1 - z_{16E})$$

$$h_W = H_1 - H_{12W} = \alpha\left(\frac{V_1^2}{2g} - \frac{V_{12W}^2}{2g}\right) + (y_1 - y_{12W}) + (z_1 - z_{12W})$$

where V designates an average flow velocity, y is an average depth, and z is an average elevation. A velocity correction coefficient $\alpha = 1.04$ was used. Subscripts 1, 16E, and 12W refer to the model stations at which y and z were measured (Fig. 13). In the prototype these stations represent the beginning and the end of the diversion structure, respectively. The value of y used was actually an average of 12 measurements taken near the designated cross section. Table D-3 in Appendix D and Figs. H-1 and H-2 give the actual values of the headlosses and the loss coefficients.

The values of λ_E and λ_W can be expected to be functions of the flow distribution between the two branches, Q_E/Q_T; the flow depth at station 1 relative to the height of the baffle piers, y_B/y_1; and the inlet Froude number Fr_1 because of the formation of some kind of undular hydraulic jump at large flow rates. Table D-3 also gives values of Q_E/Q_T, y_B/y_1, and Fr_1 as shown below.

Because a major portion of the total energy loss in the diversion structure is induced by the sudden expansion of the cross-sectional area and the baffle blocks, headloss coefficients λ_E and λ_W were graphed as a function of the Froude number Fr_1; $Fr_1 = V_1/\sqrt{gy_1}$ where V_1 is the average velocity at station 1 and y_1 is the depth at the same station. As expected, headloss coefficients are larger for higher Froude numbers Fr_1. Relative heights of the baffle blocks y_B/y_1 and relative flows, Q_E/Q_T, were fairly constant, because water depths and flow rates had been specified. Changes in the value of either parameter will also affect the values of the headloss coefficients λ_E and λ_W.

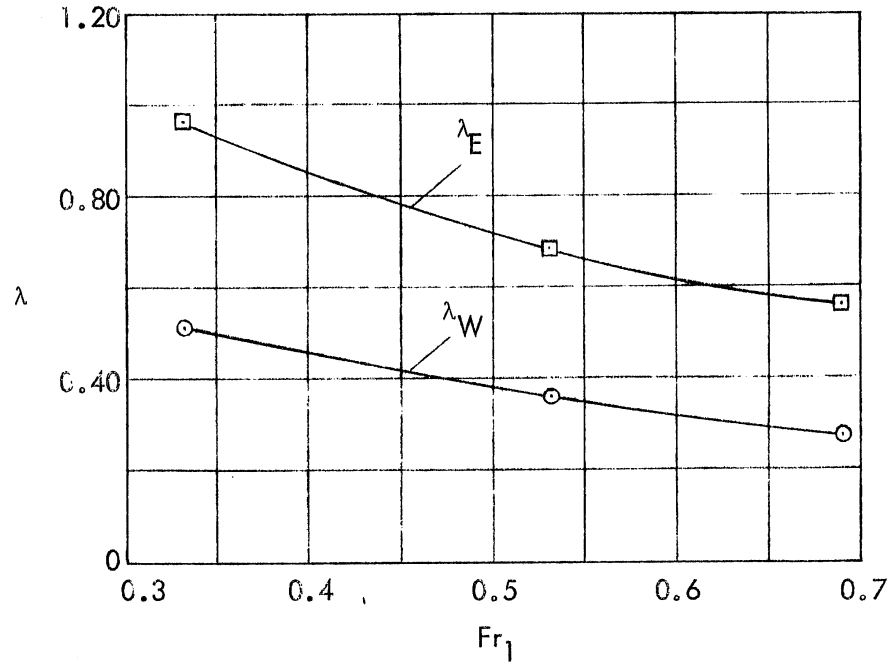

Fig. H-1 - Headloss Coefficient λ versus Froude Number at Station 1, Fr_1

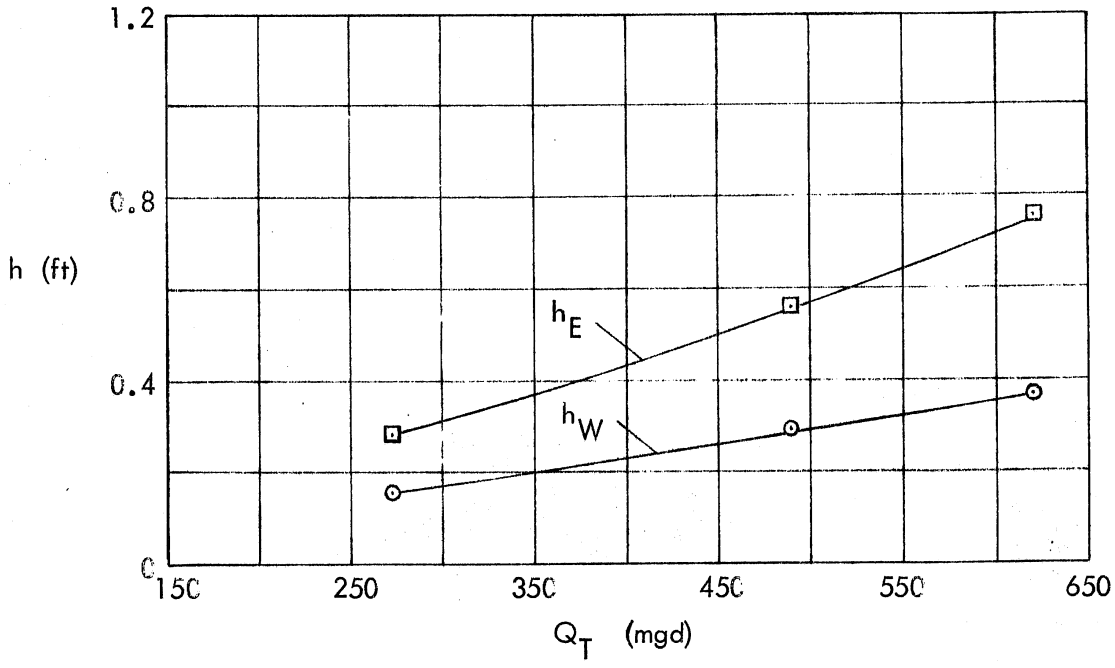

Fig. H-2 - Headloss h versus Total Discharge Q_T

4. Pier Configuration

In the design of diversion structures several elements have significance for sediment transport. These include the angle between the diversion channel, the pier configurations, and the length of the structure.

In the early stages of the model planning, some consideration was given to the effect of angle and length on the grit transport process. Comparison of the proposed design with documented similar diversion structures led to the preliminary conclusion that the bed load transport pattern would probably not be significantly affected if the diversion angle were steeper and the diversion structure shorter than proposed.

However, it was determined in the model study that, for hydraulic reasons, neither the length of the structure nor the angle proposed in the original design should be increased. In fact, the length proposed for the structure was too short to produce an acceptable flow configuration, and baffle blocks had to be installed to improve the situation.

The downstream pier is in such a position that the total available cross section is divided in portions of 60 and 40 per cent, which represent approximately the distribution of flow rates before a third barrel is added.

With the baffle blocks installed, the flow past the piers is quite satisfactory. The surface flow patterns made visible by confetti streaks in Fig. P-1 and the bottom currents indicated by the sediment streaks in Fig. P-2 for a 273 mgd flow are quite acceptable. Changes in pier length cannot be expected to improve the situation.

Fig. P-1 - Surface Flow Pattern past Piers at 273 mgd as made visible by Confetti Streaklines

Fig. P-2 - Bottom Flow Pattern past Piers at 273 mgd as made visible by Sediment Streaks

VII. SUMMARY

A physical model study was conducted to evaluate the flow of water and grit through the projected main interceptor diversion structure at the Minneapolis-St. Paul Metropolitan Sewage Treatment Plant. A physical model was built at a scale of 1:12 and tested for flow conditions ranging from 176 mgd to 930 mgd. A distribution of the flow in proportions of nearly 58 and 42 per cent was imposed. Various kinds of grit were used in the model. Water surface profiles, flow rates, grit transport rates, and headlosses were measured in the model, and the results are reported herein. In addition, the grit deposition patterns to be expected in the prototype were documented photographically and by bed profile measurements.

Six series of experiments were conducted during which the original design and several possible modifications were evaluated. A final recommended design was tested under a variety of conditions.

Hydraulic flow conditions and grit transport were used as criteria in the selection of the recommended design. The hydraulic flow conditions had to be considered as carefully as the grit transport associated with them to assure satisfactory performance of the structure. It was desired that 50 per cent or more of the total grit load be directed toward the new treatment facility. The model study conducted leads to the conclusion that the proposed modified structure will be able to produce this result while maintaining good hydraulic flow conditions for flows up to 620 mgd in two barrels or 930 mgd in three barrels. The changes recommended in the design of the structure are listed in the next section.

VIII. RECOMMENDATIONS

On the basis of laboratory findings, the following recommendations are made:

1. No sills need be placed on the floor of the diversion structure to direct the grit toward the new treatment facility if 70 per cent (or more) of the grit load is to be diverted.

2. It is necessary to install baffle blocks in the diversion structure to produce acceptable water depths and flow velocities at a total flow of 620 mgd. It is recommended that six circular baffle piers 2.5 ft in diameter and 2.5 ft high be installed at the 49.25 ft station. Figure III-1 shows the details of such placement.

REFERENCES

[1] Portland Cement Association, Handbook of Concrete Culvert Pipe Hydraulics, 1964.

[2] Silberman, E. and Paintal, A. S., A Model Study of the Grit Chambers of the Minneapolis-St. Paul Sanitary District Plant, Project Report No. 87, St. Anthony Falls Hydraulic Laboratory, Univ. of Minnesota, January 1967.

[3] ASCE, Sewage Treatment Plant Design, Manual of Engineering Practice - No. 36, 1959.

[4] Anderson, A. G., "Sedimentation," Chapter 18, Handbook of Fluid Dynamics, edited by V. L. Streeter, McGraw-Hill, 1961.

[5] Yoshimi, Y. and Stelson, T. E., "Grit Unbalance in Sewage Flow Division," Proc. ASCE, Jrl. Sanitary Eng. Division, Vol. 89, April 1963, pp. 61-85.

[6] Task Committee on Preparation of Sedimentation Manual, Committee on Sedimentation, Hydraulics Division, ASCE, Chapter V: "Sediment Control Methods: C. Control of Sediment in Canals," Jrl. Hydraulics Division, ASCE, Paper 9177, Vol. 98, No. HY9, September 1972.

[7] Mamak, W., River Regulation, published for the Department of the Interior and the National Science Foundation by ARKADY, Warsaw, Poland, 1964, pp. 95-118.

[8] Leliavsky, S., "Introduction to Fluvial Hydraulics," Chapter IX, Sediment Suspension, Dover Publications, Inc., New York, 1954, pp. 148-191.

[9] Lindner, C. P., "Diversions from Alluvial Streams," Proc. ASCE, Vol. 78, Separate No. 112, January 1952.

[10] Vogel, H. D., "Movement of Bed Load in a Forked Flume," Civil Engineering, Vol. 4, No. 2, February 1934, pp. 73-77.

[11] Vanoni, V. A.; Brooks, N. H.; and Kennedy, J. F., Lecture Notes on Sediment Transportation and Channel Stability, Rep. No. KH-R-1, W. M. Keck Laboratory of Hydraulics and Water Resources, California Institute of Technology, Pasadena, California, January 1961.

[12] Rouse, H., ed., Engineering Hydraulics, John Wiley and Sons, 1950.

LIST OF FIGURES

Fig. No.

Fig. No.

IV-4 Bed Deposits formed at 176 mgd with Grit Type 4 (Series IV)

IV-5 Oblique View of Bed Deposits shown in Fig. IV-4

IV-6 Bed Profiles of Grit Deposit - Exp. 11 - 176 mgd, type 4 grit (corn), with blocks

V-1 Water Surface Profiles along Walls of Diversion Structure - Exp. 12 - 930 mgd, no grit, with baffle blocks

VI-1 Water Surface Profiles along Walls of Diversion Structure - Exp. 14 - 620 mgd, no grit, with baffle blocks and left barrel in each downstream branch fully gated

VI-2 Water Surface Profiles along Walls of Diversion Structure - Exp. 15 - 620 mgd, no grit, with baffle blocks and right barrel in each downstream branch fully gated

VI-3 Bed Deposits formed at 620 mgd with Left Downstream Barrels Closed and Grit Type 1 (Series VI)

VI-4 Oblique View of Bed Deposits shown in Fig. VI-3

VI-5 Bed Deposits formed at 620 mgd with Right Downstream Barrels Closed and Grit Type 1 (Series VI)

VI-6 Oblique View of Bed Deposits shown in Fig. VI-5

VI-7 Bed Profiles of Grit Deposit - Exp. 16 - 620 mgd, 2 mm grit, with baffle blocks and left barrel in each branch fully gated

VI-8 Bed Profiles of Grit Deposit - Exp. 17 - 620 mgd, 2 mm grit, with baffle blocks and right barrel in each branch fully gated

H-1 Headloss Coefficient λ versus Froude Number at Station 1, Fr_1

H-2 Headloss h versus Total Discharge Q_T

P-1 Surface Flow Pattern past Piers at 273 mgd as made visible by Confetti Streaklines

P-2 Bottom Flow Pattern past Piers at 273 mgd as made visible by Sediment Streaks

APPENDIX A

Prototype Data

Table A-1 - SELECTED JOINT INTERCEPTOR FLOWS AT DIVERSION STRUCTURE, METROPOLITAN WASTEWATER TREATMENT PLANT

Condition	Description	Flows (mgd)			Flow Depth at Diversion Structure (ft)
		Total	West (old)	East (new)	
A	Total annual average flow (1980)	273	116	157	5.5
B	Maximum 3 consecutive days' flow (1980)	490	208	282	6.2
C	Minimum 1-day flow (1980)	176	70	106	5.2
D	Flow during rainfall and thaw periods (present interceptor capacity)	620	262	358	6.5
E	Flow during rainfall and thaw periods (possible future interceptor capacity)	930	262	668	7.7

Table A-2 - FLOW CHARACTERISTICS IN ONE BARREL OF EXISTING MAIN INTERCEPTOR

Flow Conditions		A[1]	B[1]	C[1]	D[1]	E[2]
Flow rate	Q (mgd)	136.5	245	88	310	310
	Q (cfs)	211.5	379.75	136.4	480.5	480.5
Depth at diversion	d (ft)	5.5	6.2	5.2	6.5	7.7
Cross section	A (ft^2)	52.25	58.90	49.4	61.75	73.15
Wetted perimeter	P (ft)	20.5	21.9	19.9	22.5	24.9
Avg flow velocity	V (ft/sec)	4.04	6.44	2.76	7.78	6.56
Hydr. radius	R_h (ft)	2.54	2.68	2.48	2.74	2.93
Hydr. diameter	D_h (ft)	10.16	10.72	9.92	10.96	11.72
Froude number	$Fr = \frac{V}{\sqrt{gd}}$	.304	.456	.213	.537	.417
Reynolds number	$Re = \frac{VD_h}{\nu}$	2.93×10^6[3]	4.93×10^6	1.96×10^6	6.10×10^6	5.49×10^6
Friction factor	f	.016[4]	.016	.016	.016	.016
Avg bed shear stress	τ_s (lbs/ft^2)	.0623	.161	.0295	.235	.167

[1] Total flow divided between two approach barrels

[2] Total flow divided among three approach barrels

[3] At water temperature of 50°F

[4] At absolute roughness of 0.004 ft

Table A-3 - SHEAR STRESS CHARACTERISTICS IN PROTOTYPE

Flow Condition:		A	B	C	D	E
Avg. bed shear stress	τ_s (lbs/ft^2)	.0623	.161	.0295	.235	.167
Grit particle size:						
--Largest size (after Shields)	d_{100} (mm)	3	8	2	12	8
--Smallest size (from Fig. 3)	d_5 (mm)	.15	.15	.15	.15	.15
Critical tractive force:						
--for largest particle	$\tau_{c,100}$	.0623	.161	.0295	.235	.167
--for smallest particle	$\tau_{c,5}$	.003	.003	.003	.003	.003
Shear stress ratios:						
--for largest particle	$\tau_s/\tau_{c,100}$	1	1	1	1	1
--for smallest particle	$\tau_s/\tau_{c,5}$	21.1	53.4	9.8	78.5	55.6

APPENDIX B

Model Data

Table B-1 - FLOW CHARACTERISTICS IN MODEL OF MAIN INTERCEPTOR

Flow Conditions		A	B	C	D	E
Flow rate	Q (cfs)	.424	.761	.273	.963	.963
Depth	d (ft)	.458	.517		.542	.642
Cross section	A (ft^2)	.363	.409		.429	.508
Wetted perimeter	P (ft)	1.708	1.825		1.875	2.075
Avg flow velocity	V (ft/sec)	1.166	1.859		2.246	1.894
Hydr. radius	R_h (ft)	.212	.223		.228	.244
Hydr. diameter	D_h (ft)	.847	.893		.913	.977
Froude number	$Fr = \frac{V}{\sqrt{gd}}$	.304	.456		.537	.417
Reynolds number	$Re = \frac{VD_h}{\nu}$ [1]	1.41×10^5	2.37×10^5		2.93×10^5	2.64×10^5
Friction factor	f [2]	.0165	.015		.0144	.0147
Avg bed shear stress	τ_s (lbs/ft^2)	.00535	.0126		.0177	.0128

[1] At water temperature of 33°F

[2] For smooth surface

APPENDIX C

Listing of Experiments

Table C-1 - LISTING OF EXPERIMENTS CONDUCTED

Series No.	Exp. No.	Flow Cond.[1]	Grit Type[2]	Measurements Made[3]
I	1	D	1	(W),(G),(D)
	2	D	2	(W),(G),(D)
	3	A	3	(W)
II	4	D	1	(W),(G),(D)
III	5	D	1	(W),(G),(D)
	6	D	2	(W),(G),(D)
	7	D	4	(G)
IV	9	B	4	(W),(G)
	10	A	4	(W),(G)
	11	C	4	(W),(G),(D)
	13	A	1	(G)
V	12	E	4	(W),(G)
VI	14	D	4	(W),(G),(Q)
	15	D	4	(W),(G),(Q)
	16	D		(G),(D)
	17	D		(G),(D)

[1] Flow conditions are defined in Appendix A (Table A-1)

[2] Grit types are defined in Fig. 12

[3] (W) - Water surface profiles
(G) - Grit flow rates
(D) - Deposition patterns
(Q) - Discharge distribution

APPENDIX D

Listings of Grit Flow Rates, Headlosses, and Headloss Coefficients

Table D-1 - MEASURED RELATIVE GRIT DISTRIBUTION

Discharge (mgd)	Grit Type	Volume - per cent West (old)	Volume - per cent East (new)
620	1	0	100
620	4	26	74
490	4	23	77
273	4	15	85

Table D-2 - MEASURED RELATIVE GRIT DISTRIBUTION

Discharge (mgd)	Grit Type	Volume - per cent West (old)	Volume - per cent East (new)
Left Barrels Fully Gated:			
620	4	15	85
Right Barrels Fully Gated:			
620	4	6	94

Table D-3 - HEADLOSS IN DIVERSION STRUCTURE ($\alpha = 1.04$)

Exp. No.	Q_T mgd	Energy Head in ft[1] H_1 ft	H_{12W} ft	H_{16E} ft	Headloss in ft h_W (old) ft	h_E (new) ft	Loss Coeff. λ_W	λ_E	Q_E/Q_T[2]	y_B/y_1[3]	Fr_1
					Two Approach Barrels:						
5	620	6.85	6.48	6.09	0.37	0.76	0.27	0.56	57.7	0.455	0.689
9	490	6.42	6.12	5.86	0.30	0.56	0.36	0.68	57.6	0.446	0.531
10	273	5.49	5.34	5.21	0.15	0.28	0.51	0.96	57.5	0.480	0.332
					Three Approach Barrels:						
12	930	7.83	7.62	7.06	0.21	0.77	0.25	0.92	71.7	0.357	0.480
					Left Barrel in each branch Fully Gated:						
14	620	8.23	7.49	7.71	0.74	0.52	1.01	0.71	54	0.333	0.432
					Right Barrel in each branch Fully Gated:						
15	620	8.47	7.68	7.47	0.79	0.99	1.17	1.47	51	0.321	0.409

1) With reference to bed at Station 1

2) Q_E = flow rate through east (new) branch
Q_T = total flow rate in both branches

3) y_B = height of the baffle blocks
y_1 = water depth at Station 1